

DEPARTMENT OF PHYSICS
UNIVERSITY OF JYVÄSKYLÄ
RESEARCH REPORT No. 2/2010

Point-defect mediated diffusion in intrinsic SiGe-alloys

BY
IIRO RIIHIMÄKI

Academic Dissertation
For the Degree of
Doctor of Philosophy

To be presented, by permission of the
Faculty of Mathematics and Natural Sciences
of the University of Jyväskylä,
for public examination in Auditorium FYS-1 of the
University of Jyväskylä on February 18, 2010
at 12 o'clock noon



Jyväskylä, Finland
February, 2010

Preface

The work reviewed in this thesis was carried out during the years 2003-2009 at the Department of Physics, University of Jyväskylä.

First of all, I want sincerely to thank my supervisor Prof. Jyrki Räisänen for making this work possible by providing me with not only much appreciated guidance, but also the chance to work with state-of-the-art experimental equipment. Another very important person for me during these years has been Dr. Ari Virtanen, whose research group I joined during this study. Thanks to him, I have been able to enjoy unlimited academic freedom and participate in several projects unrelated to this study, giving me a chance to develop my understanding in several different fields of physics. I would also like to thank Prof. Rauno Julin who got me finally interested in physics during his lectures by showing how even the very complicated topics can be made easy and accessible by common sense only. I am also thankful to many of my fellow students, but especially to Dr. Pauli Laitinen and Dr. Heikki Kettunen for providing me much needed guidance to the alchemy of experimental physics. Dr. Petteri Pusa I would like to thank for his help during the data analysis as well as for all the interesting and inspiring discussions we have had during these years.

You can learn much by reading books, but even more by drinking coffee with the right people. Most of my best memories are from these moments and it has been great pleasure to spend time with guys like Janne Pakarinen, Arto Javanainen, Mikko Rossi, Jani Hyvönen, Kimmo Ranttila, Ari-Pekka Leppänen, Alexandre Pirojenko, Mikko Laitinen and many others.

One of the strengths of our department are the well equipped technical and mechanical workshops and none of my experiments could ever have been realized without the help of guys like Martti Hytönen, Väinö Hänninen, Atte Kauppila and Markku Särkkä. I must also thank Anna-Liisa, Marjut and Soili for having the much needed patience to help me to keep my unorganized working life at least somewhat functional.

Last but not least I want to thank all my friends and family members for making my life just a great journey during these and all the previous years. I would like to address special thanks to my parents for teaching me by example the most important piece of information there is... “do not *believe* anything but question everything”!

Abstract

The aim of this thesis was to obtain fundamental diffusion data and to improve the understanding of point-defect mediated dopant diffusion in $\text{Si}_{1-x}\text{Ge}_x$ alloys. The thesis consists of experimental studies published in international journals and a summary section.

The experimental part consists of the following four articles: In article I, diffusion coefficients and Arrhenius parameters have been determined in relaxed intrinsic $\text{Si}_{1-x}\text{Ge}_x$ in the whole concentration range ($0 < x < 1$). In article II, diffusion coefficients and Arrhenius parameters have been determined for Ga and Sn diffusion in relaxed intrinsic and relaxed heavily p-doped germanium. In article III, diffusivity values have been determined for Ga in relaxed intrinsic $\text{Si}_{1-x}\text{Ge}_x$ in the whole concentration range at 907 °C. In article IV, diffusion coefficients and Arrhenius parameters have been determined for Si in intrinsic B20-structured FeSi. All the experiments discussed employed the modified radiotracer technique. The radioactive tracers were produced at the IGISOL facility located in Jyväskylä, Finland (^{31}Si and ^{66}Ga) and at the ISOLDE facility located in CERN, Switzerland (^{123}Sn).

In the summary section, an attempt has been made to understand the diffusion behavior of substitutionally solved group III, IV and V elements in $\text{Si}_{1-x}\text{Ge}_x$ alloys based on point-defect transport capacities and properties of point-defect-impurity interactions. The dissection is based on best available literature data as well as the data obtained during this study (articles I-IV).

Publications included in this thesis

- I I. Riihimäki, A. Virtanen, H. Kettunen, P. Pusa, P. Laitinen, J. Räisänen and the ISOLDE Collaboration, *Elastic interaction and diffusion of Sn in Si_{1-x}Ge_x systems*, Appl. Phys. Lett. **90**, 181922 (2007)
- II I. Riihimäki, A. Virtanen, S. Rinta-Anttila, P. Pusa, J. Räisänen and the ISOLDE Collaboration, *Vacancy-impurity complexes and diffusion of Ga and Sn in intrinsic and p-doped germanium*, Appl. Phys. Lett. **91**, 091922 (2007)
- III I. Riihimäki, A. Virtanen, H. Kettunen, P. Pusa and J. Räisänen, *Diffusion properties of Ga in Si_{1-x}Ge_x alloys*, J. Appl. Phys. **104**, 123510 (2008)
- IV I. Riihimäki, A. Virtanen, P. Pusa, M. Salamon, H. Mehrer and J. Räisänen, *Si self-diffusion in cubic B20-structured FeSi*, EPL, **82**, 66005 (2008)

Author's contributions in the articles:

The author was responsible for the planning and execution of the experiments and data analysis for articles I, II, III and IV. The author also wrote the first versions of these articles.

Other related articles to which the author contributed:

- V O. Koskelo, P. Pusa, J. Räisänen, U. Köster and I. Riihimäki, *Diffusion of beryllium in Ge and Si-Ge alloys*, J. Appl. Phys. **103**, 073513 (2008)
- VI P. Laitinen, A. Strohm, J. Huikari, A. Nieminen, T. Voss, C. Gordon, I. Riihimäki, M. Kummer, J. Äystö, P. Dendooven, J. Räisänen and W. Frank, and the ISOLDE collaboration, *Self-diffusion of ³¹Si and ⁷¹Ge in relaxed Si_{0.20}Ge_{0.80} layers*, Phys. Rev. Lett. **89**, 085902 (2002)
- VII P. Laitinen, I. Riihimäki, J. Räisänen and the ISOLDE Collaboration, *Arsenic diffusion in relaxed in Si_{1-x}Ge_x*, Phys. Rev. B **68**, 155209 (2003)
- VIII M. Laitinen, I. Riihimäki, Jörgen Ekman, A.R.A. Sagari, L.B. Karlsson, S. Sangynenyongpipat, S. Gorelick, H. Kettunen, H. Penttilä, R. Hellborg, T. Sajavaara, J. Helgesson and H.J. Whitlow, *Mobility determination of lead isotopes in glass for retrospective radon measurements*, Radiation protection dosimetry **131**(2), 212 (2008)

- IX O. Koskelo, J. Räisänen, U. Köster and I. Riihimäki, *Migration kinetics of ion-implanted beryllium in glassy carbon*, *Diamond and Related Materials* **17**, 1991 (2008)
- X P. Laitinen, J. Räisänen, I. Riihimäki, J. Likonen and E. Vainonen-Ahlgren, *Fluence effect on ion implanted As diffusion in relaxed SiGe*, *EPL*, **72**, 416 (2005)
- XI M. Salamon, A. Strohm, T. Voss, P. Laitinen, I. Riihimäki, S. Divinski, W. Frank, J. Räisänen, H. Mehrer, *Self-diffusion of silicon in molybdenum disilicide*, *Philosophical Magazine* **A84**, 737 (2004)

Contents

1. Introduction	1
2. Diffusion in crystalline semiconductors	5
2.1 Basics of diffusion	5
2.2 Diffusion mechanisms in crystalline semiconductors	6
2.2.1 Vacancy mechanism.....	6
2.2.2 Interstitialcy and substitutional/interstitial interchange mechanisms.....	7
2.2.3 Direct interstitial mechanism.....	8
2.2.4 Kick-out and dissociative mechanisms.....	8
2.2.5 Direct exchange mechanisms.....	9
3. Properties of SiGe alloys	10
3.1 Semiconductor properties of silicon and germanium	10
3.1.1 Band structure.....	10
3.1.2 Doping.....	12
3.1.3 Mobility.....	12
3.1.4 Fermi level.....	13
3.1.5 Point-defects.....	13
3.2 SiGe Alloy	14
3.2.1 $\text{Si}_{1-x}\text{Ge}_x$ material.....	15
3.2.2 Properties of $\text{Si}_{1-x}\text{Ge}_x$	15
4. Experimental methods	16
4.1 Radio tracer production	16
4.1.1 ISOLDE (CERN).....	16
4.1.2 IGISOL (Jyväskylä).....	17
4.2 Annealing	18
4.3 Serial sectioning by sputtering	19
4.4 Activity measurement	19
4.5 Determination of the diffusion coefficient	20
4.6 Determination of errors	21
5. Diffusion in SiGe alloy	22
5.1 Self diffusion and diffusion of native point-defects in silicon and germanium	22
5.2 Impurity diffusion in $\text{Si}_{1-x}\text{Ge}_x$	25
5.2.1 Vacancy mediated impurity diffusion.....	27
5.2.1 Interstitial mediated impurity diffusion.....	34

6. Diffusion systematics of group III, IV and V elements in $\text{Si}_{1-x}\text{Ge}_x$.....	36
<i>6.1 Diffusion statistics of group III, IV and V elements in Si.....</i>	<i>37</i>
6.1.1 Group III elements.....	37
6.1.2 Group V elements.....	38
6.1.3 Group IV elements.....	41
6.1.4 Systematics.....	42
<i>6.2 Diffusion statistics of group III, IV and V elements in Ge.....</i>	<i>43</i>
6.2.1 Group III elements.....	43
6.2.2 Group V elements.....	45
6.2.3 Group IV elements.....	47
6.2.4 Systematics.....	49
<i>6.3 Diffusion statistics of group III, IV and V elements in $\text{Si}_{1-x}\text{Ge}_x$.....</i>	<i>50</i>
6.3.1 Point-defect transport capacities in $\text{Si}_{1-x}\text{Ge}_x$	50
6.3.2 Diffusion of Si, Ge, Sn, As, Sb and Bi.....	51
6.3.3 Diffusion of Si, Ge, B, Al, Ga, In and P.....	52
6.3.4 Systematics.....	54
7. Conclusions.....	56
<i>7.1 Point-defect transport capacities.....</i>	<i>56</i>
<i>7.2 Point-defect-impurity interactions.....</i>	<i>57</i>
<i>7.3 Point-defect migration energies.....</i>	<i>58</i>
<i>7.4 Summary.....</i>	<i>60</i>
8. References.....	62

1. Introduction

When the first solid state transistor was demonstrated in 1947, probably nobody understood the revolution that was to come. In the early 1950s, germanium-based transistors quickly replaced vacuum tubes in electronic equipment due to their smaller size, lower power consumption, lower operating temperature and faster response time. However, it was only after the demonstration of Si-based integrated circuits in 1958 that the manufacturing of transistors seriously took off.

In 1960, Bell Labs fabricated the first silicon-based Metal-Oxide-Semiconductor Field-Effect Transistor (MOSFET) which soon announced its position as the fundamental switching element of digital logic in integrated circuits (IC). In 1970, IBM replaced magnetic memory with transistor-based memory [Don87] and the microprocessor was invented in the following year. The demand for integrated circuits grew quickly and in 1974 it was noted that if the electric field was kept constant when the MOSFET was shrunk, nearly every other transistor characteristic (packing density, operation voltage, power consumption, circuit delay, etc.) improved. This so-called constant electric field scaling law was published in 1974 by Dennard [Den74].

In the early 1970s, the dimensions of a transistor were still huge when compared to the atomic scale. Since miniaturization of the MOSFET increases the switching speed, it was possible to build faster integrated circuits with more transistors by just scaling the MOSFET dimensions [Den74] and during the next two decades, the number of transistors per IC grew from hundreds to millions. Since atoms unfortunately cannot be scaled, it was inevitable that the age of “easy” scaling would not last forever. Today, technology has already

reached the limits where atom size and quantum mechanical phenomena must be taken into account. For example, the thickness of the oxide layer between the gate and the channel in Intel's 65 nm generation transistors introduced in 2005 was only about 5 atomic layers thick. This represents the likely limit to which SiO₂ dielectric can be scaled [Bai04].

Despite the end of easy scaling, the number of transistors per IC has continued to follow Moore's law. The latest improvements in transistor performance have been mainly realized by introducing new high performance materials into the manufacturing process. The most important of these new materials is possibly silicon-germanium alloy. Its great potential arises from the possibility to modify its properties by altering the composition. The production of SiGe-devices is highly compatible with conventional Si-technology, making silicon-germanium also an ideal material from an economical point of view.

One of the weaknesses of silicon is the relatively low mobility of the charge carriers limiting the maximum operation frequency of Si-based transistors. Silicon and germanium, which both crystallize into a diamond structure, are completely miscible forming Si_{1-x}Ge_x solid solutions with x ranging from 0 to 1. When a thin layer of silicon is grown on top of a relaxed Si_{1-x}Ge_x layer, it adopts the larger lattice constant of Si_{1-x}Ge_x. This tensile strain splits the degeneracy of the valence and conduction bands yielding reduced scattering and lower carrier effective masses, thus increasing the mobility [Fis96, Ols05, Tak96].

Another example of the possibilities offered by Si_{1-x}Ge_x can be demonstrated in the SiGe heterojunction bipolar transistor, where higher charge carrier mobility is achieved by incorporating a non-uniform germanium concentration in the base region. These are just a few examples of the novel methods by

which transistor performance can be improved while keeping the physical dimensions intact.

Another disadvantage of silicon is its indirect band gap which prevents efficient light emission. Due to the lattice mismatch, it has not been possible to directly integrate high quality III-V-light emitters such as GaAs and AlAs in Si-based CMOS in the past. Germanium rich $\text{Si}_{1-x}\text{Ge}_x$, however, is nearly lattice matched with GaAs and AlAs and the problem can be overcome by growing a relaxed germanium rich $\text{Si}_{1-x}\text{Ge}_x$ layer between the Si substrate and the light emitting layer [Fiz92].

The manufacture of transistors is based on creating well defined n- and p-type regions in bulk silicon, by introducing group III (p-type) and V (n-type) impurities into the silicon lattice via ion implantation. To electrically activate the impurities, high temperature annealing is used to move the impurity atoms to the substitutional lattice sites. Since long-range diffusion cannot be prevented during the annealing, the diffusion properties of different elements must be known in order to achieve the desired dopant atom distributions. As the diffusion is material dependent, the new role of $\text{Si}_{1-x}\text{Ge}_x$ in advanced semiconductor manufacturing processes has generated interest in studying the diffusion properties of dopants in the $\text{Si}_{1-x}\text{Ge}_x$ system. With shrinking device size, new materials and strained structures, the diffusion processes are becoming more complicated, creating a need for better understanding at the microscopic scale.

Silicon-germanium alloys are also interesting materials for basic diffusion research. There are clear differences in the dopant diffusion in Si and Ge. By measuring the diffusivity of various elements in $\text{Si}_{1-x}\text{Ge}_x$ as a function of composition it is possible to gain information on the origin of these

differences. Such information is vital when the existing models of point-defect assisted diffusion are being improved. The aim of this thesis was to obtain fundamental diffusion data and to improve understanding of dopant diffusion in $\text{Si}_{1-x}\text{Ge}_x$.

2. Diffusion in crystalline semiconductors

2.1 Basics of diffusion

Diffusion is a process where the particles are redistributed via random motion. Fick's first law in one dimension relates the flux of atoms across a boundary to the concentration gradient, and is given by:

$$J_A = -D_A \left(\frac{\partial C_A}{\partial x} \right), \quad (2.1)$$

where D_A is the diffusion coefficient, J_A the flux and C_A the concentration of particles A . The combination of equation (2.1) and the continuity equation (2.2):

$$\frac{\partial C_A}{\partial t} = \frac{\partial J_A}{\partial x} \quad (2.2)$$

is generally known as Fick's second law:

$$\frac{\partial C_A}{\partial t} = \frac{\partial}{\partial x} \left(D_A \frac{\partial C_A}{\partial x} \right) \quad (2.3)$$

If the diffusion coefficient D_A is constant with respect to the position coordinate and concentration, Fick's second law reduces to:

$$\frac{\partial C_A}{\partial t} = D_A \left(\frac{\partial^2 C_A}{\partial x^2} \right) \quad (2.4)$$

The diffusion coefficient can now be determined by observing the time evolution of the experimental diffusion profile. In most cases, the temperature dependence of the diffusion constant D_A follows the Arrhenius law:

$$D = D_0 \exp\left(-\frac{H_a}{kT}\right), \quad (2.5)$$

where T is temperature and k the Boltzmann constant. The pre-exponential factor D_0 and the activation enthalpy, H_a , are found by fitting the equation (2.5) to the experimentally determined D values. When the Arrhenius parameters D_0 and H_a are known, Fick's second law determines the concentration $C(x,t)$ as a function of temperature.

2.2 Diffusion mechanisms in crystalline semiconductors

Fick's laws describe the redistribution of particles at macroscopic scale. At microscopic scales, diffusion in crystalline materials is very different to diffusion in gases, liquids or other less-ordered materials. In the following section, microscopic diffusion mechanisms in crystalline materials are presented.

2.2.1 Vacancy mechanism

A missing lattice atom is known as a vacancy. In the vacancy mechanism atoms diffuse by exchanging places with the vacancies (Fig. 2.1).

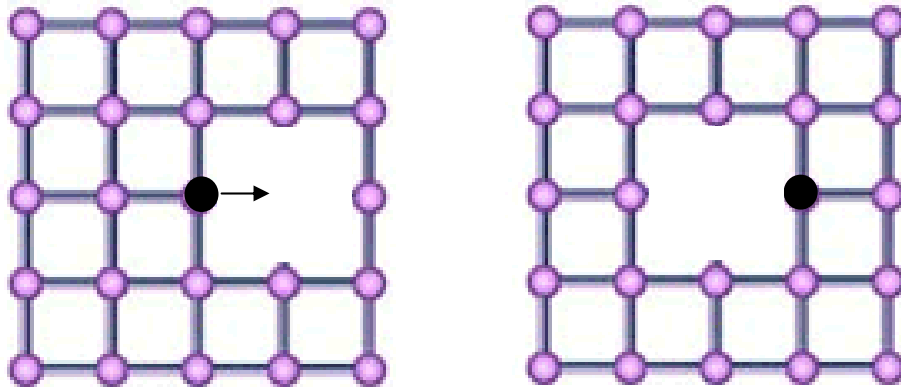


Fig. 2.1. Vacancy mechanism.

2.2.2 Interstitialcy and substitutional/interstitial interchange mechanisms

In the substitutional/interstitial interchange mechanism the diffusing atom constantly changes its position between the substitutional and interstitial lattice sites (Fig. 2.2)

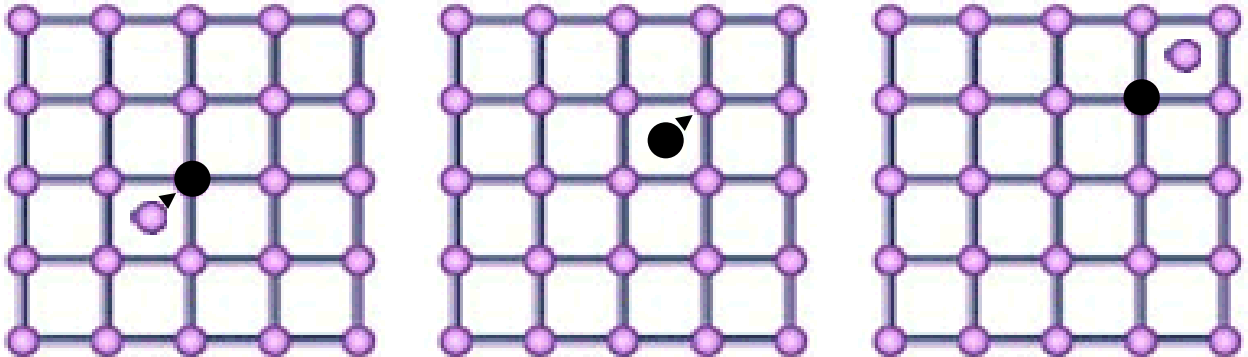


Fig. 2.2. Substitutional/interstitial interchange mechanism.

Interstitialcy is a defect where two atoms are symmetrically configured to occupy one lattice site. In the interstitialcy mechanism, one of the atoms in the interstitialcy moves towards an adjacent lattice site where it reforms the interstitialcy defect with a new host atom [Fah89].

2.2.3 Direct interstitial mechanism

In the direct interstitial mechanism an atom diffuses by jumping from one interstitial site to another (Fig. 2.3). This mechanism is typical for small atoms that occupy mainly interstitial sites.

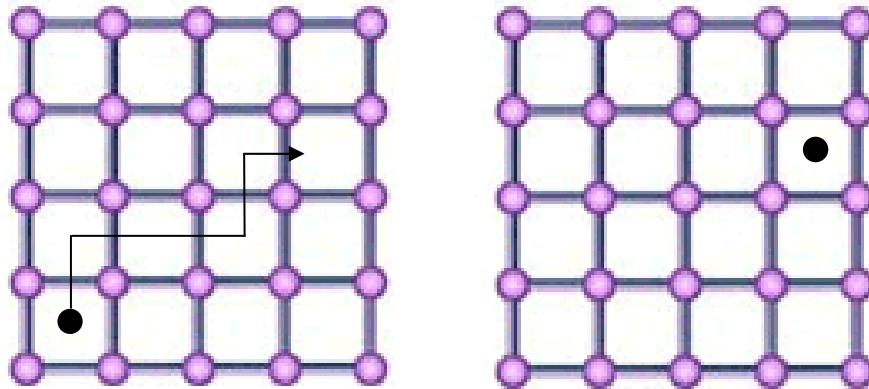


Fig. 2.3 Direct interstitial mechanism.

2.2.4 Kick-out and dissociative mechanisms

Atoms that dissolve mainly on substitutional sites but can also occupy interstitial sites may diffuse via kick-out and dissociative mechanisms. In the kick-out mechanism an atom jumps from one interstitial site to another until falling back to a substitutional position by kicking a lattice atom to an interstitial site (Fig. 2.4). The dissociative mechanism (or Frank-Turnbull mechanism) is similar to the kick-out mechanism but in this case the diffusing atom falls into a substitutional site when finding a vacancy (Fig. 2.5).

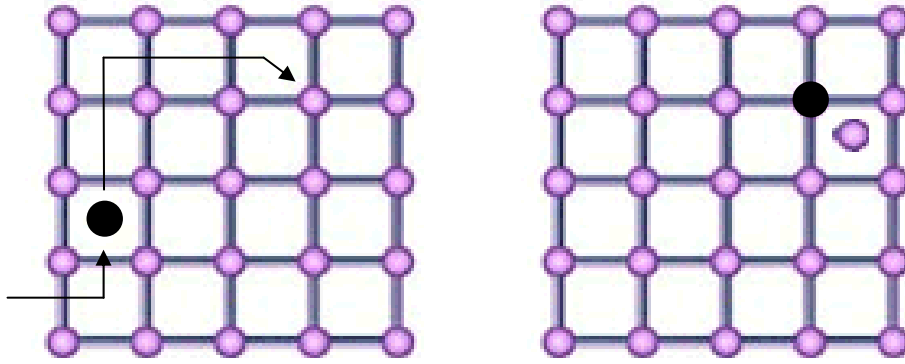


Fig. 2.4. Kick-out mechanism.

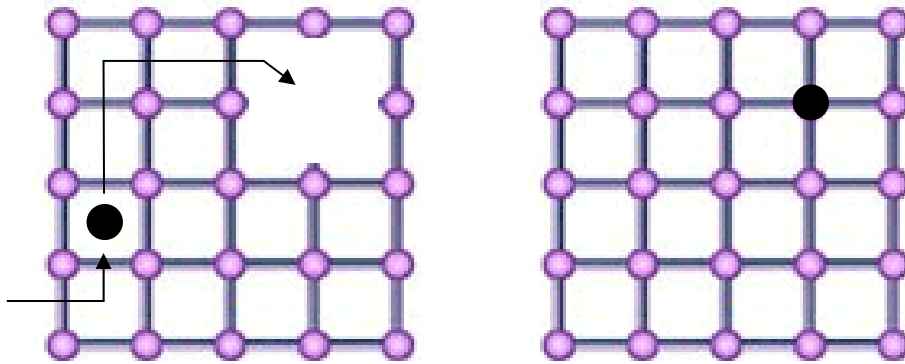


Fig. 2.5. Dissociative mechanism.

2.2.5 Direct exchange mechanisms

Diffusion could, in principle, take place via the direct exchange of two or more atoms occupying substitutional lattice sites. Experimental evidence, however, suggests that these mechanisms most probably do not have a measurable contribution to the diffusion of any element in $Si_{1-x}Ge_x$.

3. Properties of SiGe alloys

Silicon and germanium, which both crystallize into a diamond lattice, are completely miscible forming $\text{Si}_{1-x}\text{Ge}_x$ solid solutions with x ranging from 0 to 1. Most of the physical properties of $\text{Si}_{1-x}\text{Ge}_x$ change gradually from those of Si to those of Ge as the Ge concentration increases. In the following chapter the basic semiconductor properties of Si and Ge are presented, with the main emphasis being on Si.

3.1 Semiconductor properties of silicon and germanium

Table 3.1. Main physical properties of intrinsic Si and Ge at 300 K.

Material	Crystal structure	Lattice constant	Band Gap	Mobility electrons	Mobility holes	Melting point
Si	Diamond	5.431 Å	1.12 eV	$\leq 1400 \text{ cm}^2 \text{ V}^{-1} \text{ s}^{-1}$	$\leq 450 \text{ cm}^2 \text{ V}^{-1} \text{ s}^{-1}$	1412 °C
Ge	Diamond	5.660 Å	0.66 eV	$\leq 3900 \text{ cm}^2 \text{ V}^{-1} \text{ s}^{-1}$	$\leq 1900 \text{ cm}^2 \text{ V}^{-1} \text{ s}^{-1}$	937 °C

3.1.1 Band structure

The atomic numbers of silicon and germanium are 14 and 34 respectively. Si and Ge both have four of the eight allowed states in their outermost electron shell occupied. In the solid-state the close proximity of atoms leads to an overlap in the allowed energy levels and causes a splitting of each level into the allowed states multiplied by N , where N is the number of atoms in the solid, see Fig. 3.1. In case of semiconductors such as Si and Ge, the outermost energy levels form two bands referred to as the valence band and the conduction band, separated by a forbidden energy gap [Jon00].

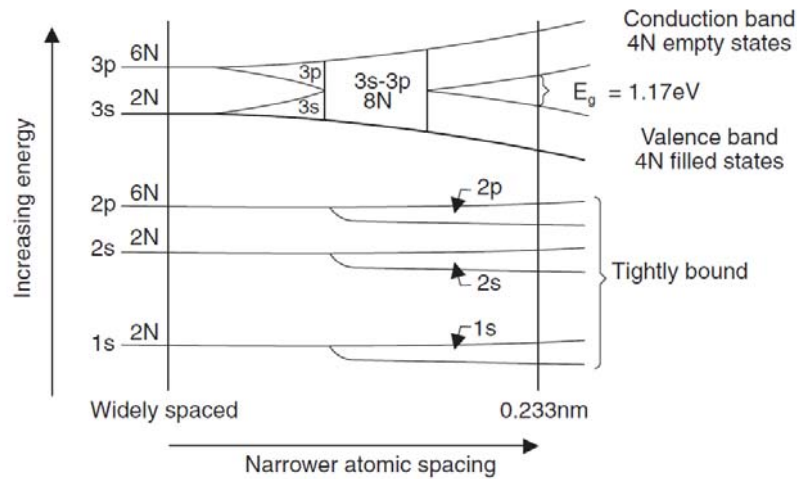


Fig. 3.1. Silicon Band structure at 300K [Jon00].

At zero Kelvin the valence band is completely filled with electrons and the conduction band completely empty, meaning that each lattice atom share electrons with the four nearest neighbor atoms forming covalent bonds. At finite temperature, some bonds are broken due to the thermal energy and subsequent electrons become mobile carriers (bond breaking means excitation from valence band to conduction band). The intrinsic carrier concentration in Si as a function of temperature is presented in Fig. 3.2.

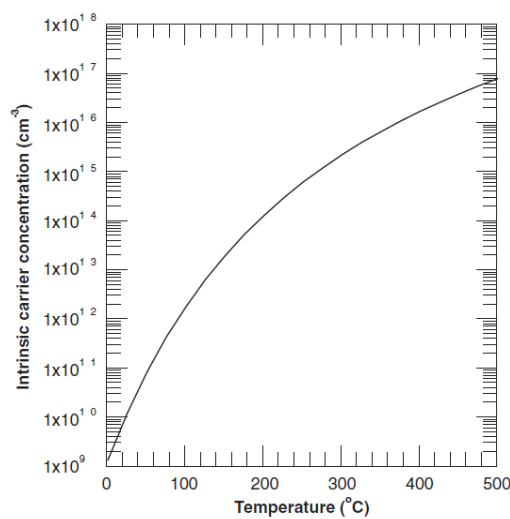


Fig. 3.2. Temperature dependence of intrinsic carrier concentration in silicon [Jon00].

3.1.2 Doping

The electrical properties of Si and Ge can be altered by introducing impurities into the lattice in a process referred to as doping. The group V elements have one electron more and the group III elements one electron less than Si and Ge in their outermost energy level. The extra electron introduced by group V elements is only weakly bound to the impurity and is therefore easily excited to the conduction band. On the other hand, introducing a group III impurity into a Si or Ge lattice forms an unfilled energy level just above the valence band. Due to the small energy gap, it is easy for electrons from the valence band to fill the newly-formed energy level. The hole left behind is now free to move through the valence band and to act as a positive charge carrier. When the concentration of charge carriers introduced by doping exceeds the intrinsic carrier concentration, the semiconductor is said to be extrinsic (n-type if the majority charge carriers are electrons and p-type if they are holes).

3.1.3 Mobility

The conduction band electrons and the valence band holes can move relatively freely around the semiconductor lattice. When an electric field is applied, the charge carriers will achieve an average drift velocity as a result of the acceleration and deceleration caused by the field and the scattering events, respectively. The rate at which the charge carriers move under the influence of the electric field is called mobility. For the low electric fields the relation can be written as

$$v_d = \mu E , \quad (3.1)$$

where v_d is the drift velocity, μ the mobility and E the strength of the electric field. Mobility itself is a function of the carrier effective mass and the mean scattering time.

3.1.4 Fermi level

The probability of finding an electron in a particular energy state E is given by the Fermi-Dirac distribution function.

$$f(E) = \frac{1}{e^{(E-E_f)/kT} + 1}, \quad (3.2)$$

where k is the Boltzmann constant, T is the absolute temperature and E_f is the Fermi level. The Fermi level is the energy level at which the probability of an energy state to be occupied by an electron is exactly one-half. In intrinsic Si and Ge the Fermi level is located approximately at the center of the band gap. In extrinsic material it is defined by the doping conditions.

3.1.5 Point defects

The native point defects, vacancies and interstitials/interstitialcys create energy levels in the band gap and can become charged by capturing electrons or holes. The formation energy of the charged point defects depends on the Fermi level. Their concentration relative to the concentration of neutral point defects, which is independent of the Fermi level, can be calculated using the following relations [Sho57, Fah89]:

$$\begin{aligned}
C_X^- &= C_X^0 \exp\left[-\frac{E_X^- - E_f}{kT}\right] \\
C_X^{\cdot} &= C_X^0 \exp\left[-\frac{E_X^- + E_X^{\cdot} - 2E_f}{kT}\right] \\
C_X^+ &= C_X^0 \exp\left[-\frac{E_f - E_X^+}{kT}\right] \\
C_X^{++} &= C_X^0 \exp\left[-\frac{2E_f - E_X^{++} - E_X^+}{kT}\right]
\end{aligned}
\tag{3.3}$$

where C represents the concentration, X the type and $-$ and $+$ signs the charge state of the point defect. E_X^- , E_X^{\cdot} , E_X^+ and E_X^{++} are the energy levels associated with the charge transitions between X^0 and X^- , X^{\cdot} and X^- , X^0 and X^+ , and X^+ and X^{++} respectively.

3.2 SiGe Alloy

There is no substructure in $\text{Si}_{1-x}\text{Ge}_x$ and as the binary phase diagram (Fig. 3.3.) indicates, Si and Ge are completely miscible in the whole composition range.

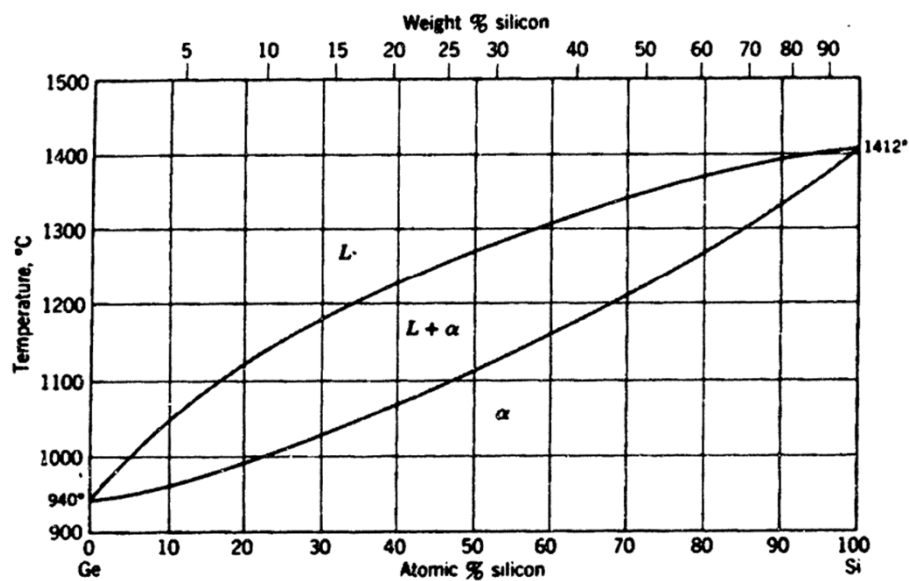


Fig. 3.3. Si-Ge Binary Phase Diagram [Gha94].

3.2.1 Si_{1-x}Ge_x material

The bulk growth of compositionally uniform Si_{1-x}Ge_x crystals is still challenging [Yon04] but by using epitaxial methods, high quality Si_{1-x}Ge_x layers of any composition can be grown upon Si substrates [Lei98]. In thin Si_{1-x}Ge_x films, the energy required for dislocations to be present to relieve the strain is larger than the strain energy accumulated in the film. As a result, a thin Si_{1-x}Ge_x layer grown on Si will adopt the lattice constant of the substrate allowing the fabrication of strained Si_{1-x}Ge_x material [Lei98]. Beyond a critical thickness, the strain energy in the film exceeds the energy necessary for formation of dislocations and the film relaxes, adopting its “normal” lattice constant. Fully relaxed Si_{1-x}Ge_x layers with the lowest threading dislocation densities can be grown by a compositional grading technique [Fiz91]. In this work, only fully relaxed Si_{1-x}Ge_x samples were used.

3.2.2 Properties of Si_{1-x}Ge_x

With the respect to diffusion, the most important properties of Si_{1-x}Ge_x are the point defect transport capacities. However, the properties of the interstitials are not well-known and one of the main goals of this study was to gain more insight into this aspect. A collection of other important Si_{1-x}Ge_x properties can be found for example in the NSM Archives [NSM].

4. Experimental methods

The diffusion experiments included in this thesis were all carried out using the radio tracer technique. Tracers with a short half-life enable diffusion experiments with peak tracer concentrations in the range of $1 \cdot 10^{11} - 1 \cdot 10^{15}$ atoms/cm³. The superb sensitivity of the radio tracer technique makes it easier to maintain the intrinsic conditions. High sensitivity is also useful in cases where the element under study has low solid solubility. The basic principles of the radio tracer technique are presented in Fig. 4.1.

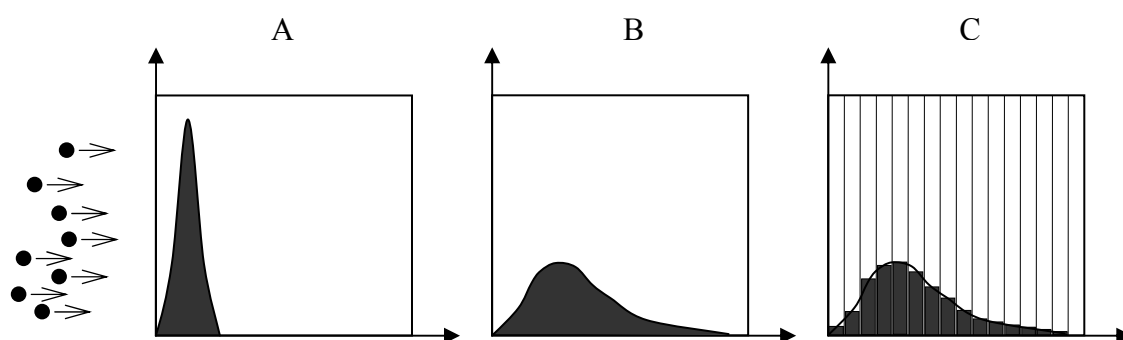


Fig. 4.1. Experimental steps of the radio tracer technique (production and implantation of the radioactive tracer (A), annealing (B) and profile construction by serial sectioning (C)).

4.1 Radio tracer production

Two facilities using the Isotope Separator On-Line (ISOL) technique were used for the production and deposition of radioactive tracers. The functional principles of these facilities are explained below.

4.1.1 ISOLDE (CERN)

At the ISOLDE mass separator facility located in CERN Switzerland, the radioactive nuclei are produced via spallation, fission or fragmentation

reactions by guiding an external proton beam with an energy of 1 or 1.4 GeV into a “thick” piece of heated target material (Uranium carbide in the experiments performed for Articles I and III]). Due to the high temperature, the reaction products diffuse out of the target material and are guided into an ion source via a transfer tube. After ionization, the radioactive nuclei are reaccelerated and mass separated after which they are implanted into the diffusion samples.

Although practically all radioactive isotopes useful for diffusion experiments are produced in ISOLDE targets, not all of them can be reaccelerated. The main bottleneck at ISOLDE is the drift time from the target to the ion source. After diffusing out of the target, the radioactive atoms must still effuse into the ion source via a transfer tube. In this process the atoms will hit the tube walls several times. If the sticking time (time that it takes for an atom to be released from the wall) is too long, no activity is left to be ionized and reaccelerated. The sticking time is a function of the tube material and the temperature as well as the properties of the traveling atom/molecule. The longest sticking times usually belong to the transition elements with high melting points.

4.1.2 IGISOL (Jyväskylä)

At the IGISOL (Ion Guide Isotope Separator On –Line) facility located in Jyväskylä Finland, radioactive nuclei are produced by using stable ion beams provided by the K-130 cyclotron and a thin target. Nuclear reactions take place in the target from which the radioactive product nuclei recoil out as an ion into a chamber filled with helium gas. During the slowing down process, a highly charged radioactive nucleus collects electrons from the He atoms until

it is thermalized and reaches a charge state of $2+$ (the first ionization energy of helium is higher than the second ionization energy of most elements). Due to charge exchange reactions with impurities such as O_2 , N_2 and H_2O , most of the product nuclei pick up one electron more, ending up with $1+$ charge state before the continuous He flow carries them through the nozzle, first to reacceleration and then to mass separation. Finally the radioactive nuclei are implanted into diffusion samples. The basic principle of the IGISOL technique is presented in Fig. 4.2.

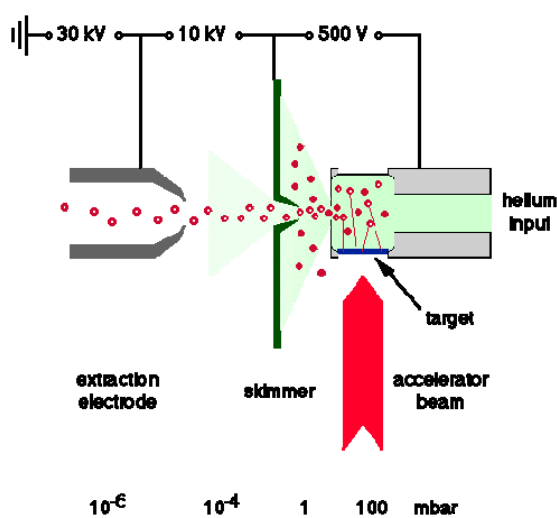


Fig. 4.2. Production, thermalization and reacceleration of the radioactive nuclei at the IGISOL facility.

At IGISOL, no ion source is needed and since the interactions of the He-gas and the reaction products only depend on the ionization energies, transition elements with high melting points can also be reaccelerated.

4.2 Annealing

The tracer implanted samples were annealed in a GIRO high temperature resistance furnace at temperatures between 575 and 1200 °C. Harmful surface reactions were minimized by using a protective gas (argon) or high vacuum

conditions (10^{-8} - 10^{-9} mbar). To further prevent surface contamination, a protective cap made from sample material was placed on top of the sample in all cases. During annealing, the temperature was monitored using thermocouples attached to the sample holder. For short annealing times, heating and cooling corrections were calculated according to the method described in Ref. [Ita74].

4.3 Serial sectioning by sputtering

The samples were serial sectioned by sputtering and the sputtered material of each slice was collected on an individual piece of mylar foil. Air was used as the sputtering gas. Depth resolution was optimized by keeping the energy of the primary beam as low as 1.2 keV and the angle between the incoming beam and the normal of the sample surface at 70 degrees. To define the x-axis of the experimental profile, the beam current was monitored during the sputtering. The final depth of the sputtering crater was measured using a KLA Tencore stylus profiler.

4.4 Activity measurement

In this work, ^{66}Ga , ^{123}Sn and ^{31}Si were used as tracers. Since all of these elements decay via beta decay, the activity of the mylar foils could be measured using large area silicon detectors with an active volume thickness of 0.5 mm. To maximize the efficiency, two of these detectors were placed face to face with a separation distance of only 5 mm. To minimize the noise level, the detectors were cooled to -5 °C. Background radiation was minimized using lead shielding and unwanted counts due to muons were rejected using anticoincidence logic.

4.5 Determination of the diffusion coefficient

Once the spatial distribution of the tracer atoms (before and after annealing) is determined via serial sectioning, quantitative analysis is needed in order to obtain the diffusion coefficient D at a given temperature. If the as-implanted profile can be approximated by a Gaussian function, the following analytical solution for the concentration independent diffusion equation (2.4) exists:

$$C(x,t) = \frac{C_0}{2\sqrt{1 + \frac{2Dt}{w^2}}} \left[\begin{aligned} & \operatorname{erfc} \left(-\frac{\frac{x_c + x}{2w^2 + 4Dt}}{\sqrt{\frac{1}{2w^2} + \frac{1}{4Dt}}} \right) \exp \left(\frac{(x-x_c)^2}{2w^2 + 4Dt} \right) + \\ & k \cdot \operatorname{erfc} \left(-\frac{\frac{x_c - x}{2w^2 - 4Dt}}{\sqrt{\frac{1}{2w^2} + \frac{1}{4Dt}}} \right) \exp \left(\frac{(x+x_c)^2}{2w^2 + 4Dt} \right) \end{aligned} \right] \quad (4.1)$$

The parameter k ($-1 < k < 1$) represents different boundary conditions at the sample surface ($x=0$). If the sample surface acts as a perfect sink, $k = -1$, whereas $k = +1$ corresponds to the case of an ideally reflecting surface.

The parameters C_0 , w and x_c can be determined by fitting the Gaussian function to an as-implanted profile (when $t = 0$ and $k = 0$, equation (4.1) reduces to a Gaussian function (4.2)).

$$C(x, t = 0) = C_0 \exp \left[-\frac{(x-x_c)^2}{2w^2} \right] \quad (4.2)$$

In reality, the shape of the experimental as-implanted profile is not exactly Gaussian. Due to this fact, Eq. (2.4) was solved numerically in cases where the diffusion length was below 50 nm.

4.6 Determination of errors

Errors arise from the determination of the diffusion temperature and the time (especially during short annealing times) and in the determination of the diffusion length. A temperature correction was applied to all diffusion data by recording the actual furnace temperatures during annealing and estimating the effective temperature based on the method described in Ref. [Ita74]. Taking into account the errors in D and $1/T$, a weighted least-square cubic method, described in Ref. [Yor66] was applied to find the best slope for determining the activation enthalpies and pre-exponential factors and the corresponding standard errors.

5. Diffusion in SiGe alloy

5.1 Self diffusion and diffusion of native point defects in silicon and germanium

In a pure Si and Ge crystal the movement of vacancies and interstitials is random and the following relation coupling the tracer self diffusion to point defect diffusion, holds:

$$D_{self} = (\phi_I + 1) \left(d_I \frac{C_I}{C_S} \right) + (\phi_V + 1) \left(d_V \frac{C_V}{C_S} \right) \quad (5.1)$$

where D_{self} is the diffusion coefficient, ϕ_I and ϕ_V the correlation factors for interstitial and vacancy mediated diffusion, d_I and d_V the diffusion coefficients for interstitials and vacancies and C_i , C_v , and C_S are the interstitial, vacancy and lattice site concentrations respectively. The factors $d_x \cdot C_x / C_S$ are called the point defect transport capacities.

Bracht et al. have calculated the temperature dependence of the interstitial transport capacity in silicon using data obtained from diffusion experiments of the metallic elements, and obtained [Sto83, Bra95]:

$$d_i \cdot C_i / C_S = 2980 \exp(-4.95 \text{ eV}/kT) \text{ cm}^2 \text{ s}^{-1} \quad (5.2)$$

where T is the temperature and k the Boltzmann constant. Based on this result and the Si self diffusion data, Bracht and Haller [Bra98] obtained for the vacancy transport capacity:

$$d_v \cdot C_v / C_S = 0.92 \exp(-4.14 \text{ eV}/kT) \text{ cm}^2 \text{ s}^{-1} \quad (5.3)$$

These results indicate that at typical diffusion temperatures both interstitials and vacancies have a significant contribution to Si self diffusion. Point defect injection studies by Ural et al. [Ura99] as well as new data from Bracht et al. [Bra07], further confirm that the transport capacities for vacancies and interstitials are of the same order of magnitude in Si.

In the case of germanium, self diffusion is solely vacancy mediated [Wer85, Vog83] and the vacancy transport capacity can be extracted directly from the self diffusion data. For the interstitial transport capacity, no reliable estimations are available but based on self diffusion data it can be concluded to be clearly smaller than the vacancy transport capacity. The fact that metals such as Cu [Sto84], Zn [Alm91], Ag [Bra91] and Au [Str01] diffuse via the dissociative, rather than the kick-out mechanism further strengthens the argument of vacancy domination over the interstitials in germanium.

According to Strohm et al. [Str02], Ge diffusion is solely vacancy mediated in $\text{Si}_{1-x}\text{Ge}_x$ when $0.35 < x < 1$. Most probably the same holds for silicon, and since there is a relatively small difference in their diffusivities [Sto02, Lai02], the following approximate relation holds in Ge-rich material:

$$D_{Ge} \approx D_{Si} \Rightarrow D_{Ge} \approx (\phi_V + 1) \left(d_V \frac{C_V}{C_S} \right) \quad (5.4)$$

This means that when $0.35 < x < 1$, the diffusivity value for Ge can be used as an approximate value for the vacancy transport capacity in $\text{Si}_{1-x}\text{Ge}_x$. The properties of the interstitial transport capacity are less well known. Especially in Ge-rich $\text{Si}_{1-x}\text{Ge}_x$, it is only known that the interstitial transport capacity is smaller when compared to the vacancy transport capacity.

From a diffusion point of view the differences in point defect properties between Si and Ge are highly significant and they deserve to be examined in more detail. By using first principles calculations, Fazio et al. and Puska et al. [Faz00, Pus98] have investigated the relative volume changes for vacancies in different charge states in Si and Ge (Table 5.1).

Table 5.1. The relative volume change for vacancies in different charge states in Si and Ge [Faz00, Pus98]. $V_{rel}^i = 100(V-V_0)/V_0$, $i=Ge$ or Si . V and V_0 are calculated as the volumes of the tetrahedra formed by the four nearest-neighbor atoms of the relaxed and ideal vacancy, respectively.

Q	V_{rel}^{Ge}	V_{rel}^{Si}
(++)	-26.7	-26.1
(+)	-30.3	-39.4
(0)	-31.2	-42.4
(-)	-40.4	-55.0
(--)	-40.8	-51.9

As seen in Table 5.1, the inward relaxation (towards the vacancy) of nearest-neighbor atoms is largest for the negatively charged and smallest for the positively charged vacancies. In Ge, the inward relaxation of the neighboring atoms always increases when one extra electron is added to a vacancy. For Si the inward relaxation is largest for a singly negative vacancy. Fazio et al. [Faz00] also found that all the lattice distortions are similar in Si and Ge in the sense that the local symmetries around the vacancy, for the lowest energy structure, are the same in both materials for all charge states. This view is however not supported by some other studies [Cou05].

Si and Ge interstitials have been found to have many similarities by several studies and there seems to be a consensus that the lowest-energy configuration for the neutral interstitial in both materials is the $\langle 110 \rangle$ -dumbbell [Sil01, Jan99, Sil01, Sch89, Mor04, Bar84, Blö93, Zhu96]. However, according to the ab

initio total energy calculations by da Silva et al. [Sil01], the $\langle 110 \rangle$ dumbbell configuration in Ge is 0.65 eV lower in energy than the next lowest-energy configuration (hexagonal), whereas, according to Zhu et al. [Zhu96], in case of Si this energy difference is only 0.1 eV, suggesting that the dumbbell interstitial is more stable in Ge. Furthermore, da Silva et al. [Sil01] found that both geometrical and total charge density analyses indicate that this lowest-energy Ge interstitial is actually not a simple $\langle 110 \rangle$ dumbbell configuration but rather a four-atom ring strongly attached to the lattice (named as “kite defect”). If these findings are correct, they can at least partly explain why in Ge the interstitial transport capacity is small when compared to the vacancy transport capacity leading to vacancy-dominated self-diffusion.

5.2 Impurity-diffusion in $Si_{1-x}Ge_x$

Whereas in a pure single crystal, the movement of the point defects is totally random, this is not the case in a crystal where there are substitutional impurities. At typical diffusion temperatures, the charge states for the isolated group III and V dopants are -1 and +1 respectively, whereas the isolated Group IV impurities are neutral. This leads to a long-range Coulomb interaction between the dopants and the charged point defects. Dopants and impurity atoms may also differ in size when compared to the host atoms, causing an elastic stress to the lattice. The vacancies and interstitials also cause an elastic stress. Pairing of the dopant/impurity atoms with the point defects can either increase or decrease this stress leading to a so-called “elastic interaction” between the point defects and the dopant/impurity atoms of “wrong” size. When the point defect and substitutional impurity atom are adjacent, some rearrangement in the electronic bonds occurs leading to an extra factor in point-defect-impurity interactions. These interactions together

define the potential between the impurities and the point defects, which in turn defines the diffusivity of the different substitutionally solved elements.

Dividing the impurity-point-defect interaction into two categories is somewhat arbitrary since these interactions are not totally independent of each other (the charge state of an impurity or a point defect also effects the lattice relaxation around it). However, during this study it became clear that dividing the point-defect-impurity interaction into an elastic and a Coulombic part provides significant help when trying to understand the diffusion systematics of the substitutionally solved group III, IV and V elements in the $\text{Si}_{1-x}\text{Ge}_x$ system.

		Group		
		III	IV	V
2sp		boron 5 B 10.811	carbon 6 C 12.011	nitrogen 7 N 14.007
3sp		aluminium 13 Al 26.982	silicon 14 Si 28.086	phosphorus 15 P 30.974
4sp		gallium 31 Ga 69.723	germanium 32 Ge 72.61	arsenic 33 As 74.922
5sp		indium 49 In 114.82	tin 50 Sn 118.71	antimony 51 Sb 121.76
6sp		thallium 81 Tl 204.38	lead 82 Pb 207.2	bismuth 83 Bi 208.98

Fig. 5.1. Periodic table for group III, IV and V elements.

The concept of isolated impurity atom *size* is not evident. From a diffusion point of view, it is best defined via the elastic forces it exerts on the surrounding lattice. Höhler et al. [Höh06] have calculated the lattice relaxations of the nearest neighbors around all important group III, IV and V elements in Si and Ge with the exception of the first row B, C and N. In Si, the nearest-neighbor atoms relax outwards (away from isolated impurity

atoms) in all cases and there is a clear trend that (with one exception of Al) inside each row of the periodic table the outward relaxation increases with increasing atomic number (valence). For example, for 4sp impurities (see Fig. 5.1), the outward relaxation is smallest for the group III Ga and largest for the group V As. The only exception to this rule is Al leading to a significantly larger outward relaxation for the nearest neighbor atoms when compared to Si and P or even to 4sp Ga and Ge. Another trend visible in the data is that the outward relaxation is smallest for the 3sp impurities and increases row by row. Supporting results can be found from ref. [Roc03].

The trends are similar in Ge but due to the larger lattice constant, the nearest neighbor atoms relax inwards around all the 3sp impurities as well as around 4sp Ga. The only exception to the rule is again Al, where the inward relaxation of the nearest neighbors is smaller than for Si, P and Ga.

5.2.1 Vacancy-mediated impurity diffusion in $\text{Si}_{1-x}\text{Ge}_x$

The migration energy, i.e. the height of the potential barrier the silicon atom must overcome in order to exchange places with the vacancy, is estimated to be between 0.18 – 0.48 eV in Si, depending on the charge state of the vacancy [Fah89]. Near to the substitutional impurities, this barrier is also affected by vacancy-impurity interactions. One possible vacancy-impurity potential is presented in Fig. 5.2.

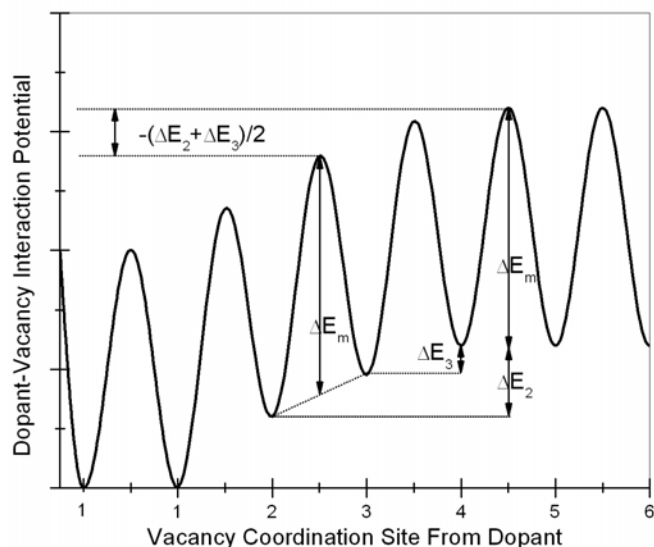


Fig. 5.2. Vacancy-dopant interaction potential as a function of coordination site in the neighborhood of a dopant.

The vacancy in a diamond lattice must visit at least the third coordination site before it can return to the impurity atom using a different path and thus cause a new diffusion jump. Due to this, the diffusivity of the substitutional impurity atom is defined by the shape and the range of the vacancy-impurity potential. The first attempt to quantitatively analyze the problem was made by Hu [Hu69, Hu73] whose analysis was later simplified by Dunham and Wu [Dun95]. For the purpose of analyzing pair diffusion, Dunham and Wu used the vacancy-dopant potential shown in Fig 5.2. Due to the attractive nature of this potential, it is more probable for a vacancy located near to a dopant atom to jump towards the dopant than away from it. This makes it highly probable that after the vacancy makes the jump from the third coordination site to the second one, it exchanges places with the dopant D at least once before reaching the third coordination site again. The reasoning above made Dunham and Wu to argue that, in the case of a long range attractive potential, the diffusivity of the dopant D is proportional to the fraction of vacancies in the third coordination site and the rate of hopping of those vacancies into the

second coordination site. They start from a basic formula for hopping diffusion:

$$D = \alpha^2 v_{\text{eff}} / 6 \quad (5.5)$$

where $\alpha = \sqrt{3} \cdot a/4$ is the jump distance (a is the size of the cubic cell), $v_{\text{eff}} = f \Sigma v_j$ is the effective mean hopping rate when each dopant hop is assumed to be uncorrelated to previous hops, f is the correlation factor and v_j are the rates of possible hops. After taking into account the lattice structure, properties of the vacancies and the shape of the dopant-vacancy potential, Dunham and Wu conclude with the following relation:

$$D = \alpha^2 \left(\frac{C_V^0}{C_S} \right) v_V^0 \exp\left(\frac{\Delta E_2 + \Delta E_3}{2kT} \right) \quad (5.6)$$

where C_V^0/C_S is the fraction of the lattice sites occupied by vacancies (far away from any impurity) and v_V^0 the hopping rate for those vacancies. ΔE_2 and ΔE_3 are the binding energies of the dopant-vacancy pair when the vacancy is in the second- or in the third-coordination site away from the dopant respectively.

The Dunham-Wu pair-diffusion model can be used to explain the diffusion enhancement caused by a long range attractive vacancy-impurity potential. It also highlights the important role of the vacancy jumps between the second and the third coordination sites. Its use, however, is limited. As will be shown later, short range elastic effects, not taken into account by the Dunham-Wu model, most probably have a role to play even in the effective E-center diffusion of the group V elements.

Due to the nature of vacancy mediated diffusion in the diamond lattice, the diffusivity of a substitutional impurity can be significantly enhanced only if the range of the attractive vacancy-impurity potential reaches at least the third coordination site [Hu69, Hu73]. On the other hand, an increase in the first-neighbor exchange barrier (EB) alone can be sufficient to significantly retard or even effectively block the vacancy mediated diffusion of a substitutional impurity (see Fig. 5.3). The role of the first-neighbor exchange barrier in diffusion of substitutionally solved impurities in Si is discussed in ref. [Nel98].

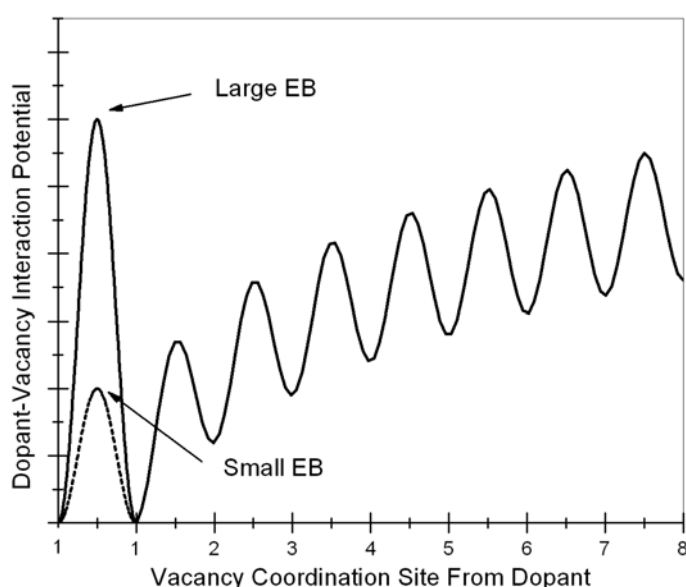


Fig. 5.3. Vacancy-dopant interaction potential as a function of coordination site and the role of first neighbor Exchange Barrier (EB).

When combining the results obtained by Nelson et al. [Nel98] and Höhler et al. [Höh06], it can be seen that there is a strong correlation between the height of the EB and the size of the isolated impurity, size being defined via the lattice relaxation of the nearest neighbors [Höh06]. The reason behind this correlation can be understood by studying the geometry of the vacancy-impurity pairs.

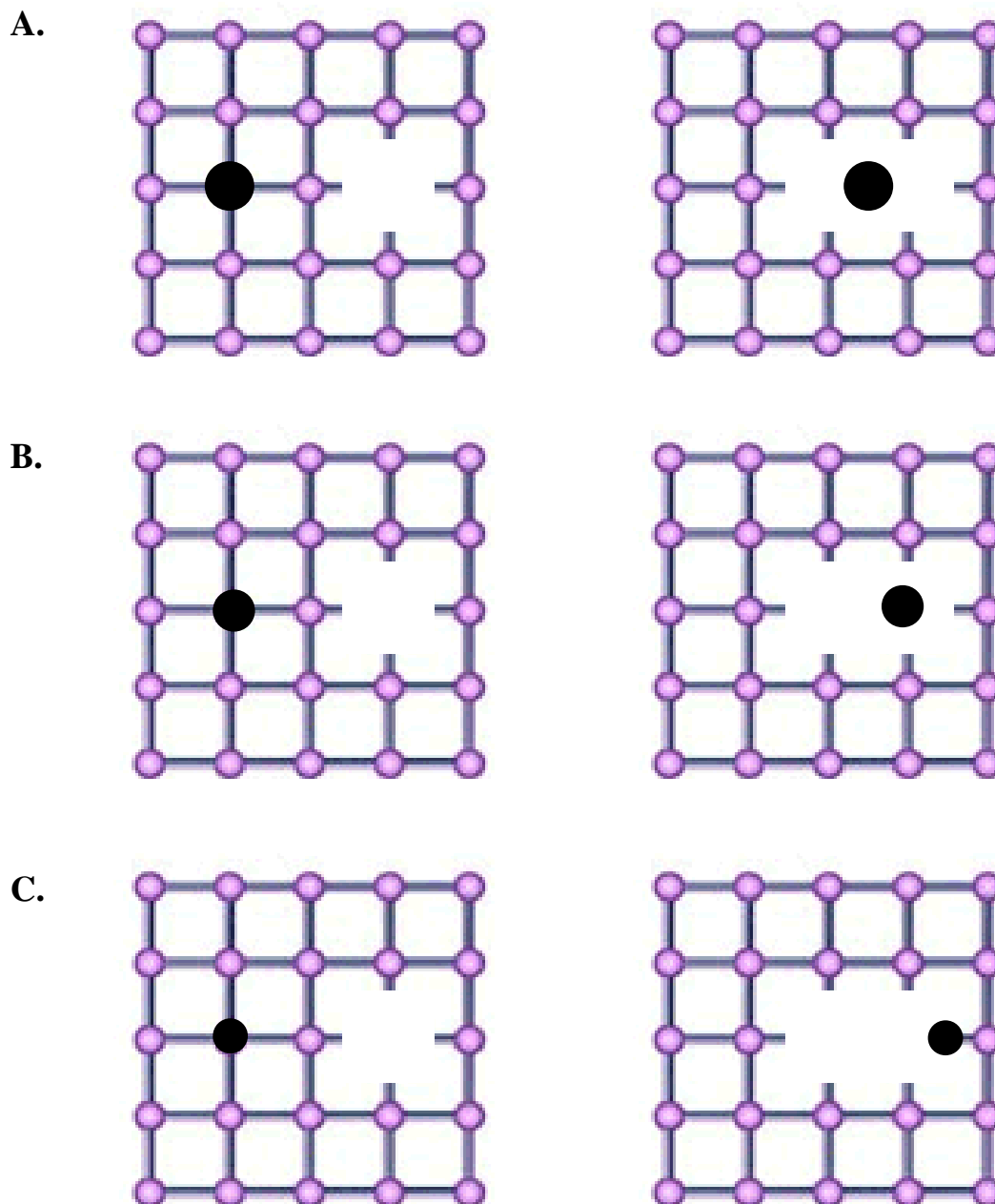


Fig. 5.4. Simplified 2D presentation of the different vacancy-impurity pair geometries (lattice relaxations are ignored). A. Impurity at bond center (split vacancy configuration). B. Impurity slightly relaxed towards the vacancy. C. Impurity relaxed away from the vacancy.

According to Höhler et al. [Höh06], EB is negative (saddle-point geometry) in Si as well as in Ge for all the studied 5sp impurities (In, Sn and Sb) and for Bi (6sp) leading to a split vacancy configuration in case of these elements (case A in Fig. 5.4). Surprisingly, in Si also Al relaxes to the bond center position. In silicon, P, Ge and As relax towards the vacancy (case B in Fig. 5.4)

whereas Ga relaxes slightly away from it. In germanium, Al, Si, P, and As relax towards the vacancy and Ga again slightly away from it [Höh06]. In Si, the small first row elements B, C and N all relax strongly away from the vacancy [Nel98] (case C in Fig. 5.4). Based on these results and on the calculations by Nelson et al. [Nel98], it can be concluded that the EB increases with an increasing jump distance, leading to a large EB for the small atoms relaxing away from the neighboring vacancy, and to a small EB for the larger atoms relaxing towards the neighboring vacancy.

The calculations by Nelson et al. [Nel98] show that in some cases, the EB can be an order of magnitude higher compared to a normal migration energy barrier seen by a Si vacancy. In these cases, it is clear that it is the EB and not the shape of the vacancy-impurity potential beyond the second coordination site that dictates the diffusivity of the substitutional impurity. For example, for B in Si the calculated value for the EB is 2.49 eV leading to exceptionally high activation energy for the vacancy-mediated diffusion [Nel98].

Based on the work of Nelson et al. [Nel98] and Höhler et al. [Höh06] it can be concluded that the diffusivity of substitutional impurities is defined not only by long range interactions, but also by size-dependent short range elastic effects dictating the height of the first neighbor exchange barrier (EB). The work of Ramanarayanan et al. [Ram04] demonstrates how the diffusivities can be calculated using the heights of the different potential barriers as a starting point. The lack of exact numerical values for the different potential barriers prevents direct calculations of the diffusivities of all group III, IV and V elements. Our main interest, however, is not the absolute diffusivity values, but to gain better qualitative understanding of the reasons behind the differences in diffusivities of different substitutional impurities. By combining the results presented in refs. [Ram04, Dun95, Nel98, Höh06], one ends up

with the following customized model for qualitative understanding of the vacancy mediated diffusion of substitutional impurities in $\text{Si}_{1-x}\text{Ge}_x$:

1. The maximum diffusivity enhancement from the vacancy transport capacity value is defined by long range vacancy-impurity interactions.
2. For “small” atoms that relax away or only slightly towards the vacancy, the bottle neck for pair-diffusion is the high EB. This causes the vacancy to jump number of times between the first and the second coordination site as well as between the second and the third coordination site before exchanging places with the substitutional impurity.
3. For “large” atoms, preferring the bond center position, the bottleneck of pair-diffusion is the vacancy jump from the first coordination site (actually split vacancy configuration) to the second one, since this is when the energy gained when relaxing into the bond center position must be “paid back”.

In chapter 6 it will be discussed how the size and valence dependent properties of the vacancy-impurity interaction potential make it easier to understand the diffusion systematics of the group III, IV and V elements in $\text{Si}_{1-x}\text{Ge}_x$.

5.2.3 Interstitial mediated impurity diffusion

Interstitial mediated impurity diffusion can be based on kick-out, substitutional/interstitial interchange or the interstitialcy mechanism and it is often difficult to have consensus via which of these mechanisms an impurity is diffusing [Sad99, Win99, Cun06, Jun04, Bra07]. In the following, the interstitialcy mechanism will be considered, since it is most probably the mechanism responsible of at least the diffusion of Al, P, Ga, and In in silicon. A simplified, but for these purposes suitable, analysis of the interstitialcy mediated impurity diffusion is found from ref. [Fah89].

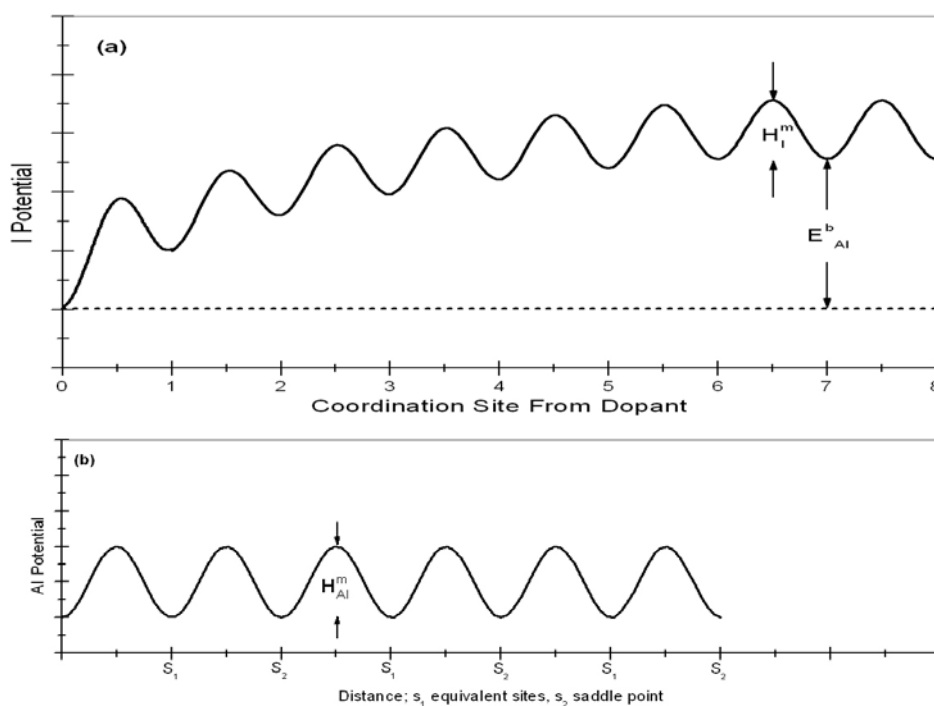


Fig. 5.5. Potential diagram for the interstitialcy mechanism: (a). formation and dissociation of the impurity-interstitialcy defect AI (containing a host atom and a substitutionally solved impurity atom). (b). migration of the impurity-interstitialcy. H_I^m and H_{AI}^m are the migration energies of the self interstitialcy and impurity-interstitialcy defect respectively and E_{AI}^b is the binding energy of the impurity-interstitialcy defect.

The shape of the long range potential between the self interstitial and the substitutional impurity (part (a) in Fig. 5.5) is defined by the Coulombic and

elastic effects. After the impurity-interstitialcy defect is formed, it is possible for the impurity to diffuse by jumping from the existing impurity-interstitialcy toward an adjacent lattice site where it re-forms the impurity-interstitialcy defect with the new host atom. This leads to an important difference between the interstitialcy and the vacancy mechanisms since, whereas the migration of an impurity atom via the vacancy mechanism requires that the diffusing defect (impurity-vacancy pair) must at least partially dissociate, the interstitialcy mechanism will operate only if the diffusing defect does not dissociate [Fah89].

The potential seen by the diffusing impurity in the most simple case is shown in part (b) of Fig 5.5. Its shape is defined by the short range interactions including the bonding effects. In real life, the shape of the potential barrier is often more complicated and may even possess some intermediate states with different charge states. There is large number of theoretical papers concerning the diffusion of B in Si but the properties of the other impurity-self-interstitial pairs are less well studied.

One interesting property of the $\text{Si}_{1-x}\text{Ge}_x$ alloy (or any binary alloy) is that the migration barriers for the vacancies and for the interstitials are not constant even in a pure material but depend on the local environment. A small difference in the diffusivity of Si and Ge suggests that in $\text{Si}_{1-x}\text{Ge}_x$, the movement of the vacancies is close to random. This, however, may not be the case for the interstitials since, according to the calculations of Wang et al. [Wan04], the presence of substitutional Ge significantly increases the migration energy of at least the Si self-interstitial.

6. Diffusion systematics of group III, IV and V elements in $\text{Si}_{1-x}\text{Ge}_x$

The intrinsic diffusivity of the group III, IV and V elements in $\text{Si}_{1-x}\text{Ge}_x$ was studied using the literature data and the data obtained during this study. The main goal is to gain understanding of the microscopic mechanisms responsible for the relative differences in the diffusivities of these elements. For some of the elements, only old and somewhat unreliable data is available making the comparisons slightly challenging.

Another problem lies in the extraction of the Arrhenius constants. If the experimental diffusivity values are measured in a short temperature range, there can be large differences in the obtained Arrhenius parameters even when the diffusivities are very similar. For example, although the differences in the diffusivities are very small, Bracht et al. have reported value of 3.42 eV for the activation enthalpy of P diffusion in Si [Bra07], whereas the value given by Zangenberg et al. is 2.8 eV [Zan03]. The reason for this discrepancy is the narrow temperature range (825-900 °C) in the Zangenberg experiment leading to a large error for activation enthalpy compensated by a lower pre exponential factor. Due to this problem, it is more reliable to compare the diffusivities of the different elements instead of the Arrhenius constants.

In the following chapter, the diffusivity values considered to be most reliable are presented. These values are selectively chosen from the literature favoring aspects such as wide temperature range, advanced experimental method and respected authors. To minimize the effect of systematic errors, for comparative purposes, data obtained by the same authors using the same experimental set up is used when possible.

6.1 Diffusion statistics of group III, IV and V elements in Si

Table 6.1. Arrhenius parameters for the group III, IV and V elements in silicon

Element	Group	Temp. [°C]	E_a [eV]	D_0 ($10^{-3} \text{ m}^2/\text{s}$)	Ref.
B	III	845-1100	3.46	0.087	[Bra07]
Al	III	850-1290	3.35	47.3	[Kra02]
Ga	III		3.51	36	[Cas75]
In	III		3.7	0.404	[Sca03]
Si	IV	855-1388	4.75	53	[Bra98]
Ge	IV	880–1270	4.83	92.3	[Kub08]
Sn	IV	950-1200	4.72	200	[Article I]
P	V	850-1100	3.42	0.075	[Bra07]
As	V	850-1100	4.2	4.7	[Bra07]
Sb	V	850-1028	4.08	2	[Nyl96]
Bi	V		4.63	103	[Cas75]

6.1.1 Group III elements

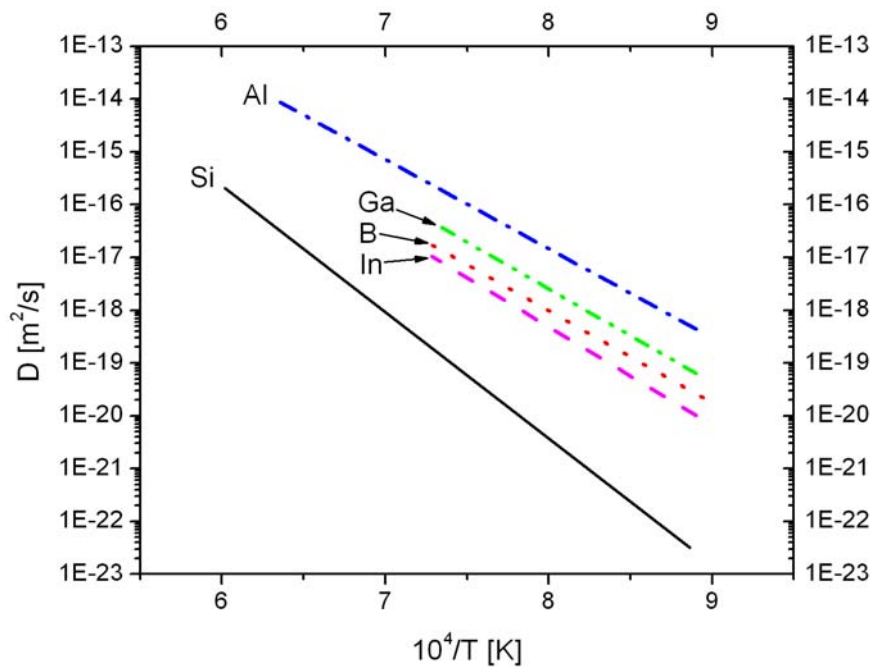


Fig.6.1. Self diffusion and the diffusion of the group III dopants in Si. References: Si (Ref. [Bra98]): black solid line, B (Ref. [Bra07]): red dotted line, Ga (Ref. [Bor88]): green dash dot dot line, Al (Ref. [Kra02]): blue dash dot line and In (Ref. [Sca03]): magenta dashed line.

According to the currently accepted interpretation, the group III dopants (B, Al, Ga, In) diffuse in Si via the interstitial mediated mechanism [Kra02, Fah89, Gro98, Bra07, Kiz96, Bon01]. Extensive studies to determine the exact microscopic mechanism have, however, only been performed for B and it is still an open question whether its diffusion proceeds via the interstitialcy or via the kick-out mechanism. Although there are many relatively recent theoretical papers suggesting the interstitialcy mediated mechanism [Sad99, Win99], the latest theoretical studies [Cun06, Jun04] along with the experimental results [Cow91, Bra07] favor the kick-out mechanism. Since it is more likely for the larger atoms to form an impurity-interstitial pair (impurity-interstitialcy defect) than an interstitial defect, the diffusion of the other group III elements is considered to proceed via the interstitialcy mechanism. As seen from Fig. 6.1, there is no correlation between the diffusivity and the size of the diffusing element in group III (even if the kick-out diffusing B is excluded). Unfortunately there is no literature data concerning the charge states or the geometries of the mobile Al, Ga and In defects preventing further speculation about the origins of the differences in their diffusivities.

6.1.2 Group V elements

For the group V dopants, there is a clear correlation between the dopant size and the fractional diffusivities (Fig. 6.2). The small-sized P atom, having an attractive elastic interaction with the interstitials, is the only group V dopant in which diffusion is dominated by the interstitial mediated mechanism in the studied temperature range [Fah89, Ura99b, Liu03]. Large Sb and Bi atoms, on the other hand, experience an attractive elastic interaction with the vacancies leading to vacancy-mediated diffusion [Dan02, Gro98, Bon01]. The diffusion of intermediate As is mediated via both, vacancies and interstitials [Ura99b].

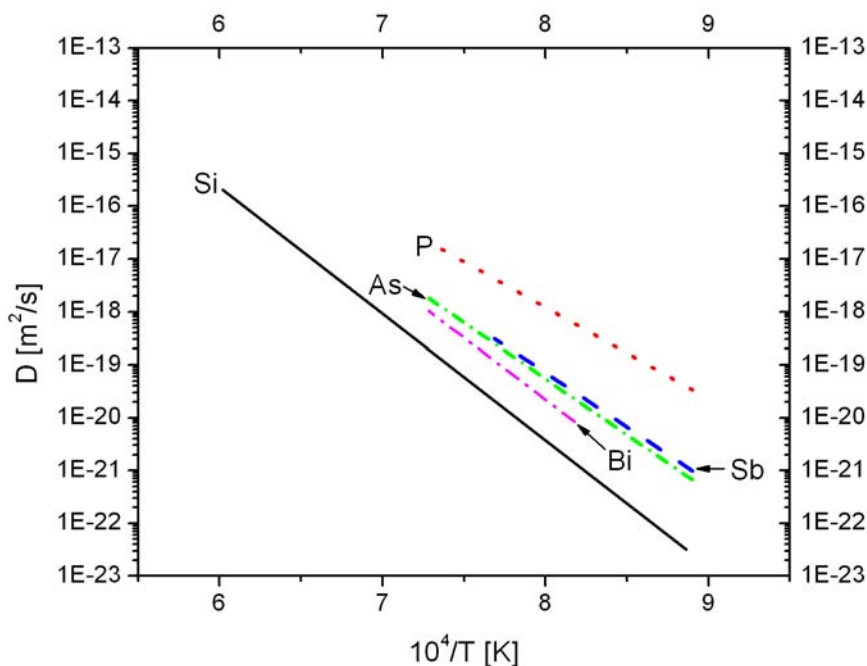


Fig. 6.2. Self-diffusion and the diffusion of the group V dopants in Si. References: Si (Ref. [Bra98]): black solid line, P (Ref. [Bra07]): red dotted line, As (Ref. [Bra07]): green dash dot dot line, Sb (Ref. [Nyl96]): blue dash dot line and Bi (Ref. [Cas75]): magenta dashed line.

The origin of the diffusion enhancement of Sb, Bi and As (vacancy component), when compared to the vacancy transport capacity, is mostly the effective pair- or E-center diffusion made possible mainly by the attractive long range Coulomb interaction between positively charged dopants and negatively charged vacancies. Since the charge state of the mobile dopant-vacancy pair is experimentally confirmed only for As (neutral) [Bra07], one may not know for sure the origin of the differences in diffusivities between As, Sb and Bi. It is, however, still worthwhile to speculate about what could be argued based on elastic effects.

As pointed out in the previous chapter, there are clear differences between the geometries of different E-centers. Large Sb and Bi atoms prefer the split vacancy configuration [Höh06] but smaller As atom relaxes only slightly towards the neighboring vacancy. Due to this, the first neighbor exchange

barrier (EB) is negative for Sb but, at least according to Nelson et al. [Nel98], as high as 0.65 eV for As. This means that for As the bottle neck of the E-center diffusion is clearly the EB whereas for Sb it is the vacancy jump from the first coordination site (actually split vacancy configuration) to the second one. The higher EB for As, together with the lower vacancy-impurity binding energy [Nel98, Höh06], could be used to explain the faster vacancy mediated diffusion of Sb when compared to the fractional vacancy component of As diffusion.

The difference in diffusivities between Sb and Bi is very interesting. Based on the experimental data obtained by Watkins et al. [Wat99] and Hirata et al. [Hir67], as well as the calculations by Höhler et al. [Höh06] and Nelson et al. [Nel98], it is clear that the vacancy-dopant binding energy is higher in case of Bi. Higher vacancy-dopant binding energy is usually thought to result in more effective pair-diffusion and thus higher diffusivity [Bro08]. However, according to the literature data, Bi diffusion is clearly slower than the diffusion of Sb (Fig. 6.2). The reason for this is probably the following; the difference in the vacancy-impurity binding energy between Sb and Bi is caused by short range elastic effects and it is mainly the potential barrier between the split vacancy configuration and the vacancy in the second coordination site that is increased due to the increase in the atom size. Despite the short range of the elastic effects, the other potential barriers are also affected, leading to a slightly higher value for the factor $(\Delta E_2 + \Delta E_3)/2$ in the case of Bi. The lower diffusivity of Bi indicates that the size dependent increase in the potential barrier between the split vacancy configuration and the vacancy in the second coordination site cannot be compensated by the slight increase in the factor $(\Delta E_2 + \Delta E_3)/2$ leading to retarded diffusion in case of Bi. Thus, if the very old and not entirely reliable data for Bi [Cas75] is

indeed correct, the slower diffusion of Bi when compared to Sb can best be understood based on the properties of short-range elastic effects.

6.1.3 Group IV elements

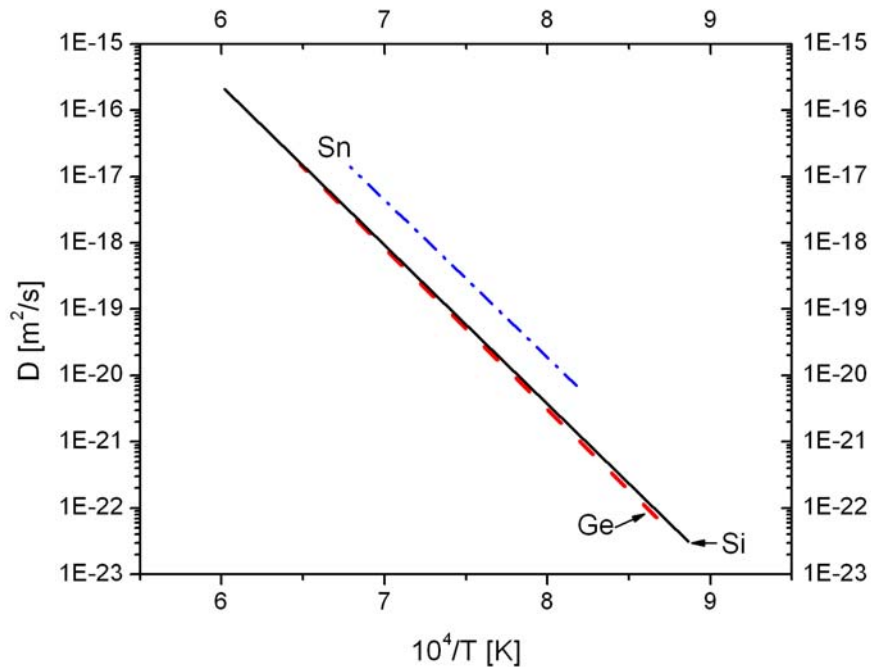


Fig. 6.3. Self-diffusion and the diffusion of the group IV impurities in Si. References: Si (Ref. [Bra98]): black solid line, Ge (Ref. [Kub08]): red dashed line, Sn (Ref. [Article I]): blue dash dot line.

The correlation between atom size and fractional diffusivities is also visible in the case of group IV elements for which the fractional vacancy component f_v is 0.4 – 0.5 for Si, 0.6 – 0.7 for Ge and close to unity for Sn [Ura99b, Fah89b, Kri97]. The absolute value of *vacancy-mediated* diffusivity (D_v , not shown in figure 6.3) also increases as a function of size (Si \rightarrow Ge \rightarrow Sn). The enhancement for vacancy-mediated Ge diffusion is still small but the difference between the diffusivity of Sn and the vacancy transport capacity is approximately an order of magnitude (Fig. 6.3). Since the isolated group IV impurities are neutral at typical diffusion temperatures, there is no long range Coulomb interaction between the Sn atom and the vacancies leaving this

difference to be explained by elastic effects. As pointed out in chapter 4, Sn prefers the split vacancy configuration indicating negative EB [Höh06, Nel98]. Since the decrease in the EB alone can, however, cause only a very limited increase in the diffusivity, the clear enhancement for the Sn diffusion when compared to the vacancy transport capacity suggests that the range of the elastic Sn-vacancy interaction potential extends at least to the third coordination site [Article II].

6.1.4 Systematics

There are two clear trends visible for the diffusion of group III, IV and V elements in Si. Firstly, although the vacancy and the interstitial transport capacities are almost equal, the diffusivity is significantly faster for elements diffusing via interstitials. This is probably caused by the fact that in the case of even the most effective E-center diffusion, the vacancy must visit at least the third coordination site between two successful diffusion jumps, making the vacancy mediated impurity diffusion less effective. In the case of the kick-out and interstitialcy mechanisms it is possible for the impurity atom to make one effective diffusion jump after another. Secondly, whereas all group III dopants diffuse via interstitials, from group V only the diffusion of the small sized P is solely interstitial mediated. Speculations about the origin of this difference/trend can be found in chapter 7.

6.2 Diffusion statistics of group III, IV and V elements in Ge

Table 6.2. Diffusion parameters for the group III, IV and V elements in germanium

Element	Group	Temp.[°C]	E_a [eV]	D_0 ($10^{-3} \text{ m}^2/\text{s}$)	Ref.
B	III	800-900	4.65	19700	[Upp04]
Al	III		3.24	16	[Cas75]
Ga	III	700-900	3.21	8	[Article II]
In	III		3.03	3.3	[Cas75]
Si	IV	550-900	3.32, 3.19	4.2, 4.3	[Sil06], [Str02]
Ge	IV	429-904	3.13, 3.14	2.54, 8.1	[Hüg08], [Str02]
Sn	IV	578-823	2.9	1.5	[Article II]
P	V	650-920	2.85	0.91	[Bro08]
As	V	640-920	2.71	3.2	[Bro08]
Sb	V	600-920	2.55	1.67	[Bro08]

6.2.1 Group III elements

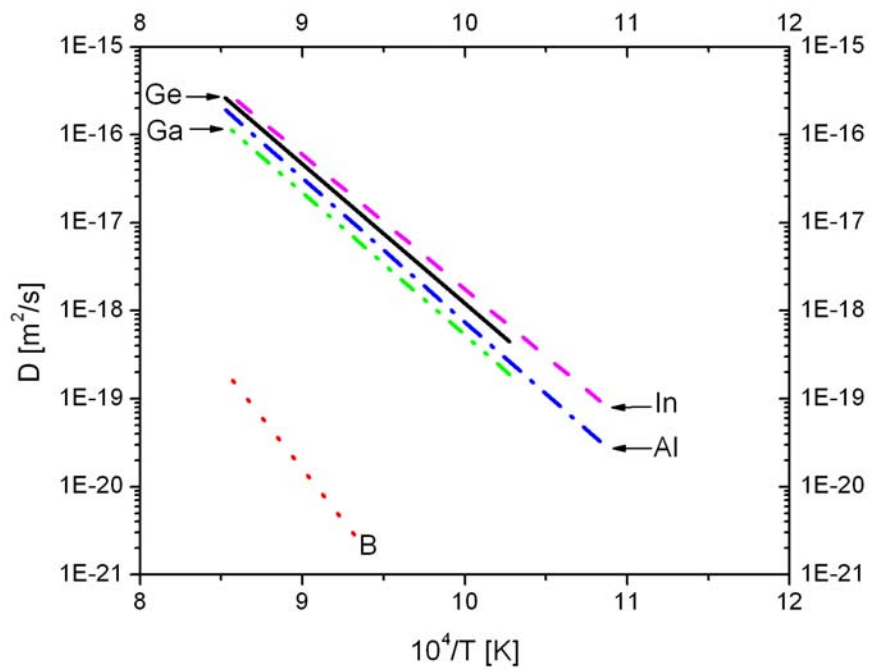


Fig. 6.4. Self-diffusion and diffusion of group III dopants in Ge. References: Ge (Ref. [Str02]): black solid line, B (Ref. [Upp04]): red dotted line, Ga (Ref. [Article II]): green dash dot dot line, Al (Ref. [Cas75]): blue dash dot line and In (Ref. [Cas75]): magenta dashed line.

In silicon, the diffusion of all group III and V dopants as well as the substitutionally solved group IV impurities was faster when compared to self-diffusion. In germanium this does not hold, the most severe example being B for which the diffusion is several orders of magnitude slower when compared to self-diffusion [Zan03, Upp01, Upp04] (Fig. 6.4). This apparent anomaly is, however, easily understood based on the properties of the vacancy-B pair. Boron, when placed next to a vacancy relaxes strongly away from it (case C in Fig. 5.4) strengthening the bonds to the remaining neighbors. Stronger bonds and longer jump distance leads to an exceptionally high EB, effectively preventing the vacancy-mediated diffusion. No calculations have been performed for the vacancy-B pair in Ge, but the effect of the small atom size on the EB can clearly be seen from the results obtained by Nelson et al. [Nel98] for the first row elements (B, C, and N) in Si. The fact that Ge self-diffusion is solely vacancy-mediated [Wer85, Vog83] shows that in Ge, the interstitial transport capacity is smaller when compared to the vacancy transport capacity, but the extremely slow diffusion of B is an indirect indicator suggesting that the difference between the transport capacities might actually be very large.

Due to the larger size of the other group III elements, there is no high EB preventing the vacancy-mediated diffusion of these elements [Nel98] and their diffusivities are similar to the self diffusion (Fig. 6.4). This lack of effective pair-diffusion suggests that for the group III elements, there is no attractive long range Coulomb force keeping the dopant-vacancy pair from dissociating. This view is supported by our finding [Article II] that at least the diffusion of Ga is practically unaffected by p-type doping indicating that the charge state of the mobile vacancy-Ga complex is the same as the charge state of an isolated Ga atom (singly negative). Werner et al. [Wer85] have also shown that the positively charged vacancies required for the effective pair diffusion

to be present for the group III elements do not play any role in the self diffusion. The lack of long range Coulomb interactions suggests that the differences in diffusivities between different group III dopants are caused by the short range elastic effects.

There are significant differences in the geometries of the group III dopant-vacancy pairs since whereas the large In prefers the split vacancy configuration (negative EB), the intermediate Al relaxes towards the vacancy and the small Ga slightly away from it [Höh06]. This makes it possible to explain the differences in their diffusivities (Fig. 6.4) on the basis of first-neighbor exchange barriers (EB) alone. This comparison is, however, quite unreliable since the differences in the diffusivities are small and some of the available data is old and unreliable (Al and In [Cas75]).

6.2.2 Group V elements

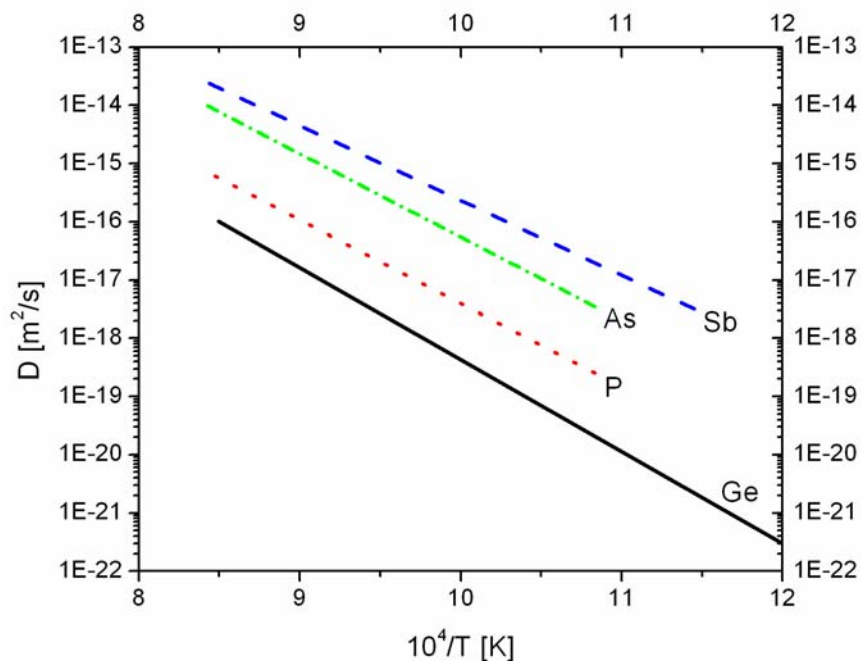


Fig. 6.5. Self-diffusion and diffusion of group V dopants in Ge. References: Ge (Ref. [Hüg08]): black solid line, P (Ref. [Bro08]): red dotted line, As (Ref. [Bro08]): green dash dot line, Sb (Ref. [Bro08]): blue dash dashed line.

The recent study by Brotzmann and Bracht [Bro08] gives a good opportunity, not only to compare the diffusivities of different group V elements in Ge, but also to see how important it is to have data obtained using the same method and experimental apparatus by the same authors before serious comparisons. Brotzmann and Bracht [Bro08] performed diffusion measurements for P, As and Sb in Ge over a wide temperature range (600 - 920 °C) using SIMS and a spreading resistance profiler. They noticed that the diffusivity increases and the activation enthalpy decreases with increasing atom size. It is, however, worthwhile to note that the trend observed by Brotzmann and Bracht is not present in some of the older data sets found in the literature [Wil67, Chu03].

The activation enthalpies extracted by Brotzmann and Bracht are 2.85, 2.71 and 2.55 eV for the P, As and Sb, respectively. Based on these results and the self diffusion data from Werner et al. [Wer85], Brotzmann and Bracht calculated the differences between the activation enthalpies of the self diffusion and the diffusion of P, As and Sb to be 0.24, 0.38 and 0.54 eV, respectively. Based on the Dunham-Wu pair diffusion model they stated that the trend is caused by the fact that the dopant-vacancy binding energy increases with increasing atom size. This interpretation, however, is not totally convincing and a better explanation can be found when the properties of the first-neighbor exchange barrier (EB) are also taken into account.

The fast E-center diffusion of all group V elements is made possible by the attractive long range Coulomb interaction between the positively charged group V dopants and the doubly negatively charged vacancies [Bro08]. Since the Coulomb parts of the dopant-vacancy interaction potential are very similar for P, As and Sb, the origin of the relatively large differences between their diffusivities is most probably elastic in nature.

Again there is a clear size-dependent trend in the geometries of the group V dopant-vacancy pairs since, whereas intermediate As relaxes more towards the vacancy than the small P, the large Sb prefers the split vacancy configuration [Höh06]. There are no EB calculations for the group III, IV and V elements in Ge but the correlation between the atom size and the height of the EB is evident when referring to the results obtained by Nelson et al. [Nel98] for silicon. The values for first-neighbor exchange barriers (EB) in Si are 1.05, 0.65 and -0.05 eV and for the dopant-vacancy binding energies 1.05, 1.17 and 1.45 eV for P, As and Sb respectively. When extrapolating these results to germanium (the trend is confirmed by Markevich et al. [Mar04]), it becomes evident that the bottleneck of the E-center diffusion is the EB at least for P (and most probably also for As), making the basic assumptions of the Dunham-Wu model incorrect. This might seem like “splitting hairs” but there is a fundamental difference between the different explanations. It is long range effects (mainly Coulombic) that keep the dopant-vacancy pairs from dissociating, but if the EB is too high (as in case of P), the vacancy spends a lot of time just “dancing” around the dopant instead of changing places with it. This leads to the argument that the origin of the large difference between the diffusivities of P and Sb is not the larger binding energy of the Sb-vacancy pair speeding up the pair-diffusion but mainly the higher EB in case of P making its E-center diffusion less effective.

6.2.3 Group IV elements

In a similar manner to group V elements, the diffusivity increases and the activation enthalpy decreases with increasing atom size (Si → Ge → Sn) also for group IV elements (Fig. 6.6). To minimize the relative errors and thus improve the reliability of the comparisons, only data obtained using the same experimental setup is used [Str02, Article II]. In this case, the same trend is

also visible if the latest available literature data from other authors is incorporated [Sil06, Hüg08, Kri94].

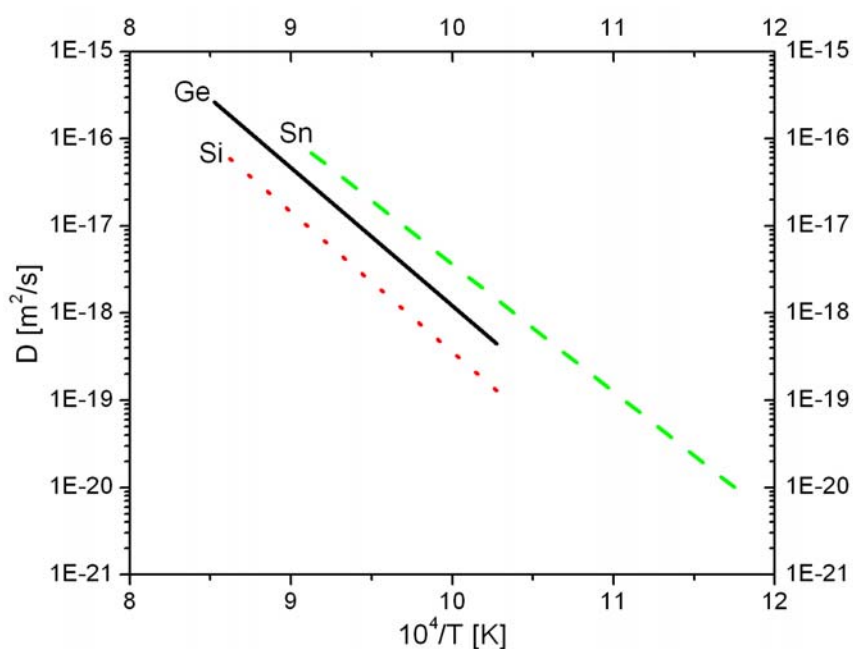


Fig. 6.6. Self-diffusion and diffusion of group IV impurities in Ge. References: Ge (Ref. [Str02]): black solid line, Si (Ref. [Str02]): red dotted line, Sn (Ref. [Article II]): green dashed line.

In germanium, Si, Ge and Sn are all pure vacancy diffusers and since the isolated group IV elements are neutral at typical diffusion temperatures, the origin of the differences in their diffusivities is most probably caused by elastic effects. In the germanium lattice, Si is slightly smaller when compared to the host atoms, leading to a repulsive interaction between the Si atoms and the vacancies. The absolute shape of the impurity-vacancy interaction potential is not known but the noted retardation of Si diffusion is most probably mainly caused by the increase in the first-neighbor exchange barrier (EB). Tin on the other hand, being larger, prefers the split vacancy configuration [Wat75, Höh06] indicating a negative EB. Since the difference in EB alone can only explain a slight diffusivity enhancement from the vacancy transport capacity value, it is argued that the clear enhancement in Sn

diffusion indicates that the range of the elastic Sn-vacancy interaction potential extends at least to the third coordination site [Article II].

6.2.4 Systematics

Self diffusion and the diffusion of boron indicate that the vacancy transport capacity in germanium is significantly higher when compared to the interstitial transport capacity. This makes germanium an ideal material to study vacancy mediated diffusion, since if one excludes the small sized boron, the differences in diffusivities of the different group III, IV and V elements are entirely caused by vacancy-impurity interactions.

Differences in the diffusivities inside each group could be well explained and understood when, in addition to the long range interactions, size-dependent differences in the first-neighbor exchange barrier (EB) and the barrier between the first- and the second coordination site are also considered. For group III elements the data are not entirely reliable but in case of the group IV and V elements, data obtained using the same experimental setup could be used.

One clear trend seen in germanium is that the diffusivity of group V dopants is significantly faster when compared to the diffusion of the group III and IV elements. This is most probably caused by the higher migration energy of the positively charged vacancies, preventing effective pair diffusion from group III elements (this topic is discussed in more detail in chapter 7).

6.3 Diffusion statistics of group III, IV and V elements in $\text{Si}_{1-x}\text{Ge}_x$

6.3.1 Point defect transport capacities in $\text{Si}_{1-x}\text{Ge}_x$

As pointed out in chapter 5, the diffusivity of germanium gives a good estimate for the vacancy transport capacity in Ge rich $\text{Si}_{1-x}\text{Ge}_x$ ($0.35 < x < 1$) (Fig. 6.7). In Si-rich material, where self diffusion is partly interstitial mediated, an approximate value for the interstitial transport capacity is known. In germanium-rich material, the only information known about the interstitial transport capacity is that it is smaller than the vacancy transport capacity.

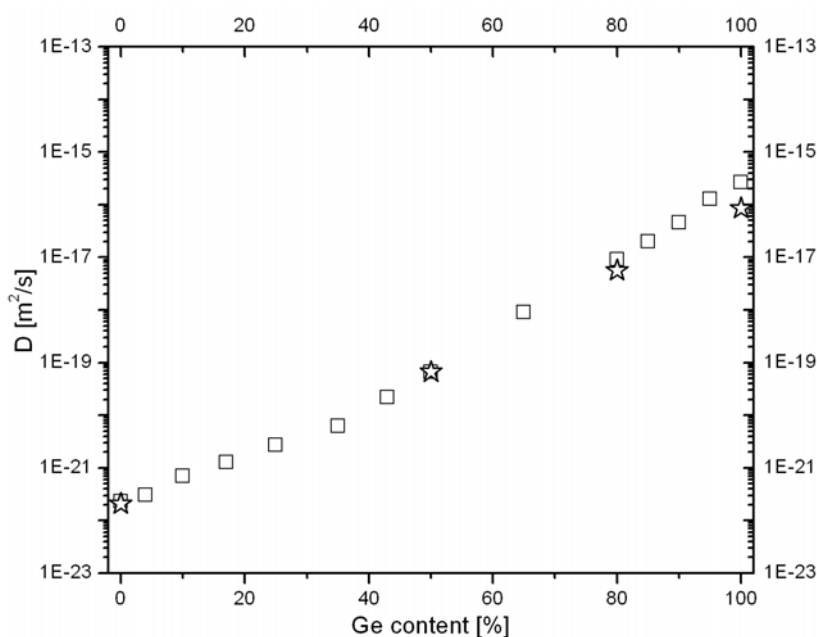


Fig. 6.7. The diffusivity of Si and Ge in $\text{Si}_{1-x}\text{Ge}_x$ as a function of the germanium content at 900 °C. References: Ge (Ref. [Sto02]): black open square, Si (Ref. [Sto02, Bra98]): black open star.

The trend visible in Fig. 6.7 reveals that in Ge-rich material ($0.35 < x < 1$), the vacancy transport capacity increases exponentially (log scale in Fig. 6.7) as a function of Ge concentration. In the following, the diffusivities of the group III, IV and V impurities are compared to the diffusivity of Si and Ge. The aim

of this comparison is to reveal to what extent the diffusivity of the different elements can be understood based on point defect properties (mainly the transport capacities).

6.3.2 Diffusion of Si, Ge, Sn, As, Sb and Bi

There are no diffusion data for Bi in $\text{Si}_{1-x}\text{Ge}_x$ but Sn and As diffusion have been measured in the whole concentration range [Article I, Lai03], and diffusion data for Sb can be found from Refs. [Nyl96, Bro08].

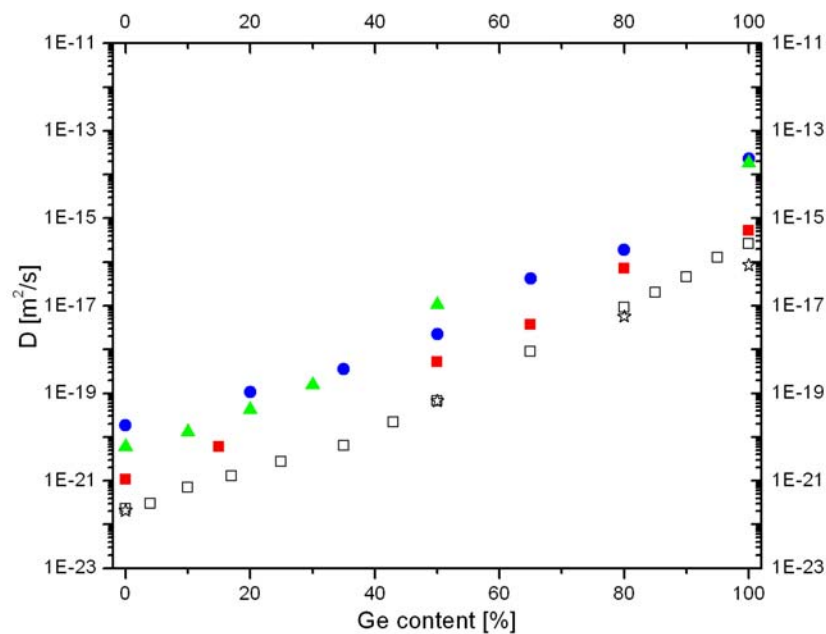


Fig. 6.8. The diffusivity of Ge, Si, Sn, As and Sb in $\text{Si}_{1-x}\text{Ge}_x$ as a function of the germanium content at 900 °C. References: Ge (Ref. [Sto02]): black open square, Si (Ref. [Sto02, Bra98]): black open star, Sn (Ref. [Article I, Article II]): red solid square, As (Ref. [Lai03]): blue solid circle, Sb (Ref. [Nyl96, Bro08]): green solid triangle.

Sn and Sb diffuse via vacancies in the whole concentration range but the diffusion of As and Ge is partly interstitial mediated when $x < 0.35$ [Lai03]. Fig. 6.8 reveals that the increase in diffusivity for As, Sn and Sb as a function of x follows the trend set by the vacancy transport capacity. Faster diffusion of Sb and As in the whole concentration range is caused by the attractive Coulomb interaction prevailing between the positively-charged group V

dopants and the negatively-charged vacancies leading to effective E-center diffusion. Also the diffusion of Sn is faster than the diffusion of Ge in the whole concentration range. In this case, the diffusion enhancement is caused by the elastic interaction leading to an attractive force between the Sn atoms and the vacancies, and to the split vacancy configuration for the vacancy-Sn pair (negative EB).

6.3.3 Diffusion of Si, Ge, B, Al, Ga, In and P

There are no data for Al and In diffusion in $\text{Si}_{1-x}\text{Ge}_x$ but the data obtained for B, Ga and P is valuable when trying to understand the evolution of point defect properties as a function of Ge concentration.

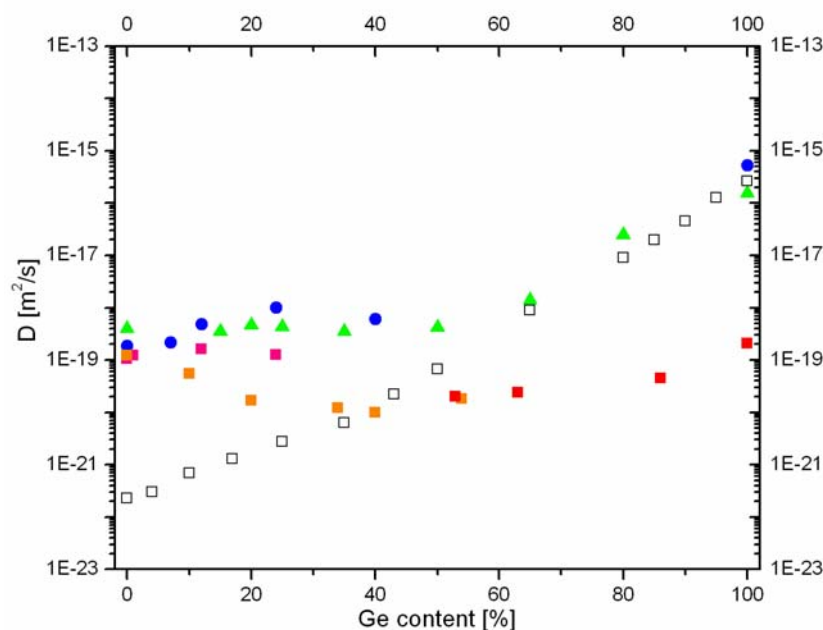


Fig. 6.9. The diffusivity of Ge, B, Ga and P in $\text{Si}_{1-x}\text{Ge}_x$ as a function of the germanium content at 900 °C. References: Ge (Ref. [Sto02]): black open square, B (Ref. [Upp03]): red solid square, B (Ref. [Kuo95]): orange solid square, (Ref. [Zan03]): pink solid square, Ga (907 °C) (Ref. [Article II, Article III]): green solid triangle, P (Ref. [Zan03, Bro08]): blue solid circle.

With the exception of B, all dopant atoms in this group diffuse via interstitials in Si and via vacancies in Ge. Boron, due to its small size, relaxes strongly

away from the neighboring vacancy leading to a longer jump distance and thus high EB [Nel98], preventing effective vacancy mediated diffusion within the whole concentration range. For the larger Ga and P this is not the case and their diffusion mechanism changes from interstitial-dominated to vacancy dominated at some Ge concentration. For the vacancy diffusers Sb, Sn and As (Fig. 6.8), it was observed that their diffusivity followed the trend set by the vacancy transport capacity all the way from Si to Ge. This indicates that there are no abrupt changes in the impurity-vacancy interactions in the whole concentration range. It is not known whether this is the case for the elements diffusing via the interstitials, but if it is so, the diffusion of B, Ga and P can reveal some of the properties of the interstitial transport capacity in Ge-rich $\text{Si}_{1-x}\text{Ge}_x$.

In Si-rich material, the diffusivity of Ga and P is close to constant, differing significantly from the trend set by the vacancy transport capacity (Fig 6.9). For P there are no data for Ge-rich material but the diffusion of Ga follows the trend set by the vacancy transport capacity when $x > 0.6$ (Fig 6.9). In a recent paper [Article III] it has been argued that the most logical way to explain this is to assume that $x = 0.6$ is the approximate concentration where Ga diffusion switches from the interstitial mediated to the vacancy mediated mode. The available data also suggests similar behavior for the diffusion of P (Fig 6.9).

The fact that in Si-rich material, the diffusion of Ga, P and B is almost concentration independent (Fig. 6.9) suggests that there is a significant difference between the behavior of the vacancy and the interstitial transport capacities in $\text{Si}_{1-x}\text{Ge}_x$. The data obtained for B indicates that this is true within the whole concentration range. Although the diffusivities of Ga, P and B follow a similar trend in Si-rich material, there are also some noted differences. Most experiments indicate that the diffusivity of B is relaxed as

well as in strained $\text{Si}_{1-x}\text{Ge}_x$ decreases as a function of Ge content up to $x = 0.4$ [Upp01, Zan01, Lev98, Fan95, Kuo93, Pai95]. The diffusivity of Ga on the other hand is almost constant and for P the increase in Ge concentration leads to a slight increase in the diffusivity. Although it is not possible to draw definite conclusions about the origin of the differences based on existing literature data alone, some speculations are still useful.

In the concentration region where the diffusion of B, Ga and P is interstitial mediated, their diffusivity is defined by the availability of self-interstitials. Since, as pointed out in section 5.2.3, in Si-rich $\text{Si}_{1-x}\text{Ge}_x$ the migration energy of Si interstitials is significantly increased by the presence of Ge atoms, the availability of Si-self interstitials is lower in regions where there is a higher concentration of Ge atoms. Furthermore, as it is energetically favorable for small-sized B atoms to be situated next to Ge atoms (due to the compensatory stress relief), they will be in contact with Si-interstitials less frequently than the larger sized Ga and P atoms. This could be one reason why the diffusivity of B decreases in Si-rich material as the Ge concentration increases whereas the diffusivities of Ga and P remain almost constant.

6.3.4 Systematics

At constant temperature, the diffusivity of purely vacancy diffusing elements such as Sb and Sn increases exponentially as a function of Ge concentration (Fig. 6.8). This trend is caused by the similar increase in vacancy transport capacity (Fig. 6.7). On the other hand, the interstitial mediated diffusion of B in $\text{Si}_{1-x}\text{Ge}_x$ (at least at 900 °C) varies only slightly as Ge content increases from 0 to 1. The most logical way to explain this is to assume that the interstitial transport capacity in $\text{Si}_{1-x}\text{Ge}_x$ is close to concentration independent.

The validity of this assumption is supported by the finding that the overall trends for the diffusivity of all the group III, IV and V elements in $\text{Si}_{1-x}\text{Ge}_x$ can be well explained and understood based on the suggested point defect transport capacities.

7. Conclusions

Point-defect mediated diffusion of impurities in crystalline materials is traditionally treated in the same way as direct interstitial diffusion ($D=D_0\exp(-H_a/kT)$). However, as pointed out by Ramanarayanan et al. [Ram04], concepts such as activation energy do not have any clear physical meaning in these more complicated processes. Vacancy-mediated diffusion of impurities, for example, depends on the properties of several different potential barriers affected by the vacancy-impurity interactions. The only way to deeply understand the origins of the differences in diffusivities of different substitutional impurities is to study the effects of point-defect-impurity interactions on these barriers.

Due to the present limitations of computational power, the exact shapes of the potential barriers cannot be calculated from first principles. However, there are clear correlation between the size of an impurity atom and the height of these potential barriers [Nel98, Höh06]. By studying these correlations, an attempt has been made in this work to understand the diffusion systematics of the group III, IV and V elements in $\text{Si}_{1-x}\text{Ge}_x$. In the following, the main results of impurity atom diffusion in SiGe alloys are shortly discussed and summarized.

7.1 Point-defect transport capacities

From the diffusion data for Si and Ge in $\text{Si}_{1-x}\text{Ge}_x$, an approximate value for the vacancy transport capacity is known for the whole concentration range and it is found to increase exponentially as a function of the Ge content. Based on the literature diffusion data for P and B along with the new data for Ga, it can

be argued that the interstitial transport capacity is most probably close to concentration-independent. The suggested properties of the point defect transport capacities would coherently explain the basic trends visible in Figs. 6.8 and 6.9.

7.2 Point-defect-impurity interactions

The fact that the diffusivity of all studied vacancy diffusing elements follows the exponential trend set by the vacancy transport capacity indicates that the relative diffusion enhancement caused by the vacancy-impurity interactions is almost constant for the whole concentration range. The case for interstitial-impurity interactions is not as clear and more experimental, as well as theoretical, data is needed before solid conclusions can be made.

According to Höhler et al. [Höh06], there is a clear correlation between the size (defined by the lattice relaxation of the nearest neighbor atoms) of an impurity and the geometry of the vacancy-impurity-pair. On the other hand, calculations by Nelson et al. [Nel98] point out that there is a strong correlation between the geometry of the vacancy-impurity-pair and the heights of the exchange barriers between the first and the second as well as the second and the third coordination site. Based on these results, realistic explanations for the differences in diffusivities of the vacancy diffusing elements with the same valence (group III, IV and V) could be generated.

The case with elements diffusing via interstitials is more difficult. All group III elements diffuse via interstitials in Si and there is no correlation between their size and their diffusivities. The lack of reliable data for the geometries

and the charge states of the mobile interstitial-dopant pairs prevents further speculation about the origins of the noted differences in their diffusivities.

Enhanced diffusion of the group V elements in both Si and Ge is known to be caused by the long range Coulomb interaction prevailing between the positively-charged dopants and the negatively-charged vacancies. Due to the lower transport capacity of the positively-charged vacancies (confirmed by self-diffusion studies), a similar enhancement is not present for the negatively-charged group III dopants. The origin of this charge-state dependence of the vacancy transport capacity has previously not been well understood.

7.3 Point-defect migration energies

As pointed out in chapter 5, there is a strong correlation between the height of the first neighbor exchange barrier (EB) and the vacancy-dopant pair geometry: The more the dopant relaxes towards the neighboring vacancy, the lower the EB becomes [Höh06, Nel98]. This is due to the decrease in the jump distance needed for the impurity to exchange places with the vacancy. For isolated vacancies, the inward relaxation of the neighboring host atoms is charge-state dependent. According to Refs. [Faz00, Pus98] (Table 5.1), inward relaxations are largest in the case of negatively-charged and smallest in the case of positively-charged vacancies in both Si and Ge, leading to longer jump distances in the case of positively-charged vacancies.

If the correlation between the jump distance and the height of the EB is also assumed to exist in case of isolated vacancies, this trend in jump distances should translate into charge-state dependent migration energies such that the migration energy would be highest for positively charged vacancies with

small inward relaxations and thus longer jump distance. There is no migration energy data for the Ge vacancies but according to Fahey et al. [Fah89] and references therein, this is indeed the case in Si since the migration energies are 0.18 eV, 0.33 eV and 0.45 eV for doubly-negative, neutral and doubly-positive charged vacancies, respectively. The trend is confirmed by Pagava et al. [Pag03]

The higher migration energy of the positively charged vacancies caused by the smaller inwards relaxation of the neighboring host atoms explains well why positively charged vacancies do not contribute to self diffusion in Si and Ge. It also explains why, in Ge, the diffusion of the group III dopants is not enhanced like the diffusion of the group V dopants and why the positively charged vacancies do not contribute to Ga diffusion even in highly extrinsic p-type conditions where their concentration is significantly increased [Article II].

In Si, where the transport capacities for both native point defects are of the same order of magnitude, the interstitial mediated diffusion of group III elements is clearly faster when compared to the purely vacancy diffusing group V elements Sb and Bi. This is most probably caused by the fundamental differences between the vacancy mechanism and interstitial mediated mechanisms. In the case of the kick-out and the interstitialcy mechanism, it is possible for the impurity to make one effective diffusion jump after another. On the other hand, in the case of even most effective E-center diffusion, the vacancy must visit at least the third coordination site between two successful diffusion jumps, making the vacancy-mediated impurity diffusion less effective.

It is still unexplained why the group V elements, with the exception of the small sized P, diffuse via vacancies rather than interstitials in Si. If the logic

used for the vacancies is applied to the interstitials, one comes to the conclusion that the migration energy is higher for the negatively-charged than the positively-charged self-interstitials. This would explain why the positively charged group V elements prefer vacancies over interstitials, although their diffusion is slower when compared to group III elements diffusing via interstitials. This view is also supported by the fact that the fractional interstitial diffusivity of As is much smaller when compared to the interstitial mediated diffusivity of the group III elements. Unfortunately these assumptions cannot be further confirmed since there are no available literature data for the migration energies of the interstitials with different charge states.

7.4 Summary

Based on existing literature data and data obtained during this thesis, it is argued that the basic diffusion behavior trends of all dopants and group IV impurities in $\text{Si}_{1-x}\text{Ge}_x$ can be reasonably explained and understood by taking into account the known point defect transport capacity properties, and the size and valence dependent point defect-impurity interactions. However, especially in Ge-rich $\text{Si}_{1-x}\text{Ge}_x$, only a limited number of experimental diffusion studies are available and to develop this concept further, more experimental as well as theoretical data is needed.

In this thesis it is suggested that not only a correlation, but also a causal relation exists between the vacancy migration energy and the inward (towards the vacancy) relaxation of the neighboring host atoms. An interesting future project would be to study this phenomenon using atomistic simulations.

At the moment impurity atom diffusion processes and the properties of point-defects are usually studied separately. However, point-defect mediated diffusion of impurities and the properties of point-defects should rather be studied as one uniform problem. The first steps toward such approach have been already taken by some research groups.

8. References

- [Bai04] P. Bai, et al, Symposium on VLSI Technology Digest of Technical Papers, 50-51 (2004)
- [Bar84] Y. Bar-Yam and J.D. Joannopoulos, *Phys. Rev. B* **30**, 2216 (1984)
- [Blö93] P.E. Blöchl, E. Smargiassi, R. Car, D.B. Laks, W. Andreoni and S.T. Pantelides, *Phys. Rev. Lett.* **70**, 2435, (1993)
- [Bon01] J.M. Bonar, A.F.W. Willoughby, A.H. Dan, B.M. McGregor, W. Lerch, D. Loeffelmacher, G.A. Cooke and M.G. Dowsett, *Journal of Materials Science: Materials in Electronics* **12**, 219 (2001)
- [Bor88] R.J. Borg and G.J. Dienes, *An Introduction to Solid State Diffusion* (Academic, London, 1988)
- [Bra95] H. Bracht, N.A. Stolwijk and H. Mehrer, *Phys. Rev. B* **52**, 16542 (1995)
- [Bra98] H. Bracht and E.E. Haller, *Phys. Rev. Lett.* **81**, 393 (1998)
- [Bra07] H. Bracht, H. H. Silvestri, I. D. Sharp and E.E. Haller, *Phys. Rev. B* **75**, 035211 (2007)
- [Bro08] S. Brotzmann and Hartmut Bracht, *J. Appl. Phys.* **103**, 033508 (2008)
- [Cas75] H. C. Casey, Jr. and G. L. Pearson, in *Diffusion in Semiconductors*, Vol. **2**, edited by J. H. Crawford and L. M. Slifkin, p. 163 (Plenum Press, New York, 1975)
- [Chu03] C.O. Chui, K. Gopalakrishnan, P.B. Griffin, J.D. Plummer and K.C. Saraswat, *Appl. Phys. Lett.* **83**, 3275 (2003)
- [Cou05] J. Coutinho, R. Jones, V.J.B. Torres, M. Barroso, S. Öberg and P.R. Briddon, *J. Phys.: Condens. Mat.* **17**, L521-L527 (2005)
- [Cow90] N.E.B. Cowern, K.T.F. Jansen, G.F.A. van de Walle and D.J. Gravesteijn, *Phys. Rev. Lett.* **65**, 2434 (1990)
- [Cun06] V. Cuny, Q. Brulin, E. Lampin, E. Lecat, C. Krzeminski and F. Cleri, *Europhys. Lett.*, **76** (5), 842 (2006)
- [Dan02] A. Dan, A.F.W. Willoughby, J.M. Bonar, B.M. McGregor, M.G. Dowsett and R.J.H. Morris, *International Journal of Modern Physics B*, **16**, Issue 28-29, 4195 (2002)
- [Den74] R. Dennard, et al., *IEEE Journal of Solid State Circuits*, vol. **SC-9**, no. 5, pp. 256-268 (1974)

- [Don87] B. Donlan and D. Pricer “Pushing the limits: Looking forward... Looking Back”, *Microelectronic Design*, Vol. **1**, (1987)
- [Dun95] S.T. Dunham and C.D. Wu, *J. Appl. Phys.* **78**, 2362 (1995)
- [Fah89] P.M. Fahey, P.B. Griffin and J.D. Plummer, *Rev. Mod. Phys.* **61**, 289 (1989)
- [Fah89b] P.M. Fahey, S. S. Iyer and G. J. Scilla, *Appl. Phys. Lett.* **54**, 843 (1989)
- [Fai81] R.B. Fair, in *Impurity Doping Processes in Silicon*, edited by F.F.Y. Wang, Chap. 7 (North Holland Amsterdam, 1981)
- [Fan95] W.T. Fang, P.B. Griffin and J.D. Plummer, *Mater. Res. Soc. Symp. Proc.* **379** (1995)
- [Faz00] A. Fazzio, A. Janotti and Antônio J.R. da Silva, *Phys. Rev. B* **61**, 2401 (2000)
- [Fis96] M.V. Fischetti and S.E. Laux, *J. Appl. Phys.*, vol. **80**, pp. 2234-2252, (1996)
- [Fit98] E. A. Fitzgerald, K. C. Wu, M. T. Currie, N. Gerrish, D. Bruce and J. T. Borenstein, *Materials Research Society Symposia Proceedings* **518**, 233 (1998)
- [Fiz91] E.A. Fitzgerald, *Appl. Phys. Lett.* **59**, 811 (1991)
- [Fiz92] E.A. Fitzgerald, Y.-H. Xie, D. Monroe, P.J. Silverman, J.M. Kuo, A.R. Kortan, F.A. Thiel and B.E. Weir, *Journal of Vacuum Science and Technology B* **10**, 1807 (1992)
- [Gha94] S.K. Ghandhi, “VLSI Fabrication Principles: Silicon and Gallium Arsenide. New York, John Wiley & Sons (1994)
- [Gro98] H. J. Grossman, “*Dopants and Intrinsic Point-Defects During Si Device Processing*,” in H. R. Huff, U. Gosele and H. Tsuya, eds. “*Semiconductor Silicon 1998*” *Electrochem. Soc. Proc.*, 98-1, (1998)
- [Hir67] M. Hirata, H. Saito and J.H. Grawford Jr., *J. Appl. Phys.* **38**, 2433 (1967)
- [Hu69] S.M. Hu, *Phys. Rev.* **180**, 773 (1969)
- [Hu73] S.M. Hu, *Phys. Status Solidi B* **60**, 595 (1973)
- [Hüg08] E. Hüger, U. Tietze, D. Lott, H. Bracht, D. Bougeard, E. E. Haller and H. Schmidt, *Appl. Phys. Lett.* **93**, 162104 (2008)
- [Höh06] H. Höhler, N. Atodiresi, K. Schroeder, R. Zeller and P.H. Dederichs, *Vacancy complexes with oversized impurities in Si and Ge*, Springer Berlin Heidelberg, p. 37-40, HFI/NQI (2004)
- [Ita74] K. Itayama and H.P. Stüwe, *Z. Metallkd.* **65**, 70 (1974)

- [Jan99] A. Janotti, R Baierle, A.J.R. da Silva, R. Mota and A. Fazio, *Physica B* **273-274**, 575-578 (1999)
- [Jon00] Scotten W. Jones, "properties of Silicon", ICKnowledge llc, http://www.icknowledge.com/misc_technology/SiliconChapter.pdf
- [Jun04] M.Y.L. Jung, R. Gunawan, R.D. Braatz and E.G. Seebaur, *AIChE Journal* **50**, 3248 (2004)
- [Kiz96] I. C. Kizilyalli, T.L. Rich, F.A. Stevie and C.S. Rafferty, *J. Appl. Phys.* **80** (9), 4944 (1996)
- [Kos08] O. Koskelo, J. Räisänen, U. Köster and I. Riihimäki. *Diamond and Related Materials* **17**, 1991(2008)
- [Kra02] O. Krause, H. Ryssel and P. Pichler, *J. Appl. Phys.* **91** (9), 5645 (2002)
- [Kri94] P. Kringhoj and R.G. Elliman, *Appl. Phys. Lett.* **65**, 324 (1994)
- [Kri97] P. Kringhoj and A. Nylandsted Larsen, *Phys. Rev. B* **56**, 6396 (1997)
- [Kuo95] P. Kuo, J.L. Hoyt and J.F. Gibbons, *Mat. Res. Soc. Symp. Proc* **379**, 373 (1995)
- [Kuo93] P. Kuo, J.L. Hoyt, J.F. Gibbons, J.E. Turner, R.D. Jacowitz and T.L. Kamins, *Appl. Phys. Lett.* **62**, 612 (1993)
- [Lai02] P. Laitinen, A. Strohm, J. Huikari, A. Nieminen, T. Voss, C. Gordon, I. Riihimäki, M. Kummer, J. Äystö, P. Dendooven, J. Räisänen and W. Frank, *Phys. Rev. Lett.* **89**, 085902 (2002)
- [Lai03] P. Laitinen, I. Riihimäki, J. Räisänen and the ISOLDE Collaboration, *Phys. Rev. B* **68**, 155209 (2003)
- [Lai05] P. Laitinen, J. Räisänen, I. Riihimäki, J. Likonen and E. Vainonen-Ahlgren. Fluence effect on ion implanted As diffusion in relaxed SiGe. *Europhysics Letters* **72**, 416(2005)
- [Lei98] C.W. Leitz, PhD Thesis (2002)
- [Lev98] R.F. Lever, J.M. Bonar and A.F.M. Willoughby, *J. Appl. Phys.* **83**, 1988 (1998)
- [Liu03] X. Liu, W. Windl, K.M. Beardmore and M.P. Masquelier, *Appl. Phys. Lett.* **82**, 1839 (2003)
- [Luo05] G. Luo, C.C. Cheng, C.Y. Huang, S.L. Hsu, C.H. Chien, W.X. Ni and C.Y. Chang, *Electron. Lett.* **41**, 24 (2005)
- [Mar04] V.P. Markevich, I.D. Hawkins, A.R. Peaker, K.V. Emtsev, V.V. Emtsev, V.V. Litvinov, L.I. Murin and L.Dobaczewski, *Phys. Rev. B* **70**, 235213 (2004)

- [Moo65] G. E. Moore, "Gramming more components onto integrated circuits", *Electronics*, Vol. **38**, N. 8, (1965)
- [Mor04] M.D. Moreira, R.H. Miwa and P. Venezuela, *Phys. Rev. B* **70**, 115215 (2004)
- [Nel98] J.S. Nelson, P.A. Schultz and A.F. Wright, *Appl. Phys. Lett.* **73** (2), 247 (1998)
- [Nic89] C.S. Nicols, C.G. van de Walle and S.T. Pantelides, *Phys. Rev. B* **40** (1989) 5484
- [NSM] Electronic archive, New Semiconductor Materials, <http://www.ioffe.ru/SVA/NSM/>
- [Nyl96] A. Nylandsted Larsen and P. Kringhoj, *Appl. Phys. Lett.* **68** (19) (1996)
- [Ols05] S. H. Olsen, M. Temple, A. G. O'Neill, D. J. Paul, S. Chattopadhyay, K. S. K. Kwa and L. S. Driscoll, *Thin Film Solids*, Vol. **508**, Issues 1-2, 5, p. 338 – 341 (2006)
- [Pag03] T. A. Pagava and Z. V. Basheleishvili, *Semiconductors*, Vol. **37**(9), 999 (2003)
- [Pai95] A.D.N. Paine, M. Morookz, A.F.M. Willoughby, J.M. Bonar, P. Phyllips, M.G. Dowsett and G. Cooke, *Mater. Sci. Forum* **196-201**, 345 (1995)
- [Pic04] P. Pichler, *Intrinsic Point Defects, Impurities and Their Diffusion in Silicon*, Springer, Vienna (2004)
- [Pus98] M. J. Puska, S. Pöykkö, M. Pesola, and R. M. Nieminen, *Phys. Rev. B* **58**, 1318 (1998)
- [Ram03] P. Ramanarayanan, K. Cho and B.M. Clements, *J. Appl. Phys.* **94**, 174 (2003).
- [Ram04] P. Ramanarayanan, B. Srinivasan, K. Cho and B.M. Clemens, *J. Appl. Phys.* **96** (12), 7095 (2004)
- [Roc03] A. Rockett, D.D. Johnson, S.V. Khare and B.R. Tuttle, *Phys. Rev. B* **68**, 233208 (2003)
- [Sad99] B. Sadigh, T.J. Lenosky, S.K. Theiss, M. Caturla, T. Dias de la Rubia and M.A. Foad, *Phys. Rev. Lett.* **83**, 4341 (1999)
- [Sal04] M. Salamon, A. Strohm, T. Voss, P. Laitinen, I. Riihimäki, S. Divinski, W. Frank, J. Räisänen, H. Mehrer. Self-diffusion of silicon in molybdenum disilicide. *Philosophical Magazine* **A84**, 737(2004)
- [Sca03] S. Scalese, M. Italia, A. La Magna, G. Mannino, V. Privitera, M. Bersani, D. Giubertoni, M. Barozzi, S. Solmi and P. Pichler, *J. Appl. Phys.* **93**(12), 9773 (2003)
- [Sch89] H.R. Schober, *Phys. Rev. B* **39**, 13013-13015 (1989)

- [Sho57] W. Shockley and J. Last, *Phys. Rev.* **107**, 392, (1957)
- [Sil00] A.R.J. da Silva, A. Janotti, A. Fazio, R.J. Baierle and R. Mota, *Phys. Rev. B* **62**, (2000) 9903-9906
- [Sil01] A.J.R. da Silva, R. Baierle, R. Mota and A. Fazio, *Physica B* **302-303**, 364-368 (2001)
- [Sil06] H. H. Silvestri, H. Bracht, J. Lundsgaard Hansen, A. Nylandsted Larsen and E.E. Haller, *Semicond. Sci. Technol.* **21**, 758-762 (2006)
- [Sto83] N.A. Stolwijk, B. Schuster, J. Hölzl, H. Mehrer, and W. Frank, *Physica B*, **116**, 335 (1983)
- [Str02] A. Strohm, T. Voss, W. Frank, P. Laitinen and J. Räisänen, *Z. Metallkd.* **93**, 737 (2002)
- [Tak96] S.I. Takagi, J.L. Hoyt, J.J. Welser and J.F. Gibbons, *J. Appl. Phys.*, vol. **80**, pp. 1576-1577, (1996)
- [Upp01] S. Uppal, A.F.M. Willoughby, J.M. Bonar, A.G.R. Evans, N.E.B. Cowern, R. Morris and M.G. Dowsett, *Physica B* **308-310**, 525 (2001)
- [Upp04] S. Uppal, A.F.M. Willoughby, J.M. Bonar, N.E.B. Cowern, T. Grasby, R. J. H. Morris and M.G. Dowsett, *J. Appl. Phys.* **96**, 1376 (2004)
- [Ura99] A. Ural, P.B. Griffin and J.D. Plummer, *Phys. Rev. B* **83**, 3454 (1999).
- [Ura99b] A. Ural, P.B. Griffin and J.D. Plummer, *J. Appl. Phys.* **85**, 6440 (1999).
- [Vog83] G. Vogel, G. Hettich and H. Mehrer, *J. Phys. C* **16**, 6197 (1983)
- [Wan04] L. Wang, P. Clancy and C. S. Murthy, *Phys. Rev. B* **70**, 165206 (2004)
- [Wat75] G.D. Watkins, *Phys. Rev. B* **12**, 4383 (1975)
- [Wat99] G.D. Watkins, in *Properties of Crystalline Silicon, EMIS data Review Series No. 20*, p. 643, edited by R. Hull (INSPEC, London, 1999)
- [Wer85] M. Werner, H. Mehrer and H. D. Hochheimer, *Phys. Rev. B* **32**, 3930-3937 (1985)
- [Wil67] G. N. Wills, *Solid-State Electron.* **10**, 1 (1967)
- [Win99] W. Windl, M.M. Bunea, R. Stumpf, S.T. Dunham and M.P. Masquelier, *Phys. Rev. Lett.* **83**, 4345 (1999)
- [Yon04] I. Yonenaga, *Journal of Crystal Growth*, Volume **275**, Issues 1-2, 91-98 (2005)

- [Yor66] D. York., Can. J. Phys. **44**(5) 1079-1086 (1966)
- [Zan01] N.R. Zangenberg, J. Fage-Pedersen, J. Lundsgaard Hansen and A. Nylansted Larsen, Defect Diffus. Forum **194-199**, 703 (2001)
- [Zan03] N.R. Zangenberg, J. Fage-Pedersen, J. Lundsgaard Hansen and A. Nylansted Larsen, J. Appl. Phys. **94**, 3883 (2003)
- [Zhu96] J. Zhu, T.D. dela Rubia, L.H. Yang, C. Mailhiot and G.H. Gilmer, Phys. Rev. B **54**, 4741 (1996)